NASA TECHNICAL NOTE

NASA TN D-4878

NASA TN D-4878

COMPRESSIVE PROPERTIES AND COLUMN EFFICIENCY OF METALS REINFORCED ON THE SURFACE WITH BONDED FILAMENTS

by George W. Zender and H. Benson Dexter

Langley Research Center
Langley Station, Hampton, Va.

NATIONAL AERONAUTICS AND SPACE ADMINISTRATION • WASHINGTON, D. C. • NOVEMBER 1968

NASA TN D-4878

COMPRESSIVE PROPERTIES AND COLUMN EFFICIENCY OF METALS REINFORCED ON THE SURFACE WITH BONDED FILAMENTS

By George W. Zender and H. Benson Dexter

Langley Research Center
Langley Station, Hampton, Va.

NATIONAL AERONAUTICS AND SPACE ADMINISTRATION

For sale by the Clearinghouse for Federal Scientific and Technical Information
Springfield, Virginia 22151 – CFSTI price $3.00

COMPRESSIVE PROPERTIES AND COLUMN EFFICIENCY OF METALS REINFORCED ON THE SURFACE WITH BONDED FILAMENTS

By George W. Zender and H. Benson Dexter
Langley Research Center

SUMMARY

Compressive tests were performed on metal tubes axially reinforced with filaments bonded to the tube outer surface. Sixty-eight magnesium, aluminum, and titanium tubes reinforced with boron or S-glass filaments were tested. The specimens consisted, by volume, of approximately 50 percent metal, 25 percent filament, and 25 percent epoxy resin. Remarkable mechanical properties indicating substantial weight-saving potential for aerospace structures were obtained. Mass-strength comparisons using the experimental results showed the boron-reinforced metals to weigh from 25 to 40 percent of the weight of titanium for compressive crushing strength and from 40 to 60 percent for column instability. Magnesium or aluminum reinforced with S-glass filaments weighs less than 50 percent of the weight of titanium for compressive crushing strength and about 70 percent for column instability.

The concept of bonding high-performance filaments to metal structures builds upon the large existing background of fabrication technology for aerospace structures. This advantage along with the potential weight saving indicated by test data suggests important practical application in structural design.

INTRODUCTION

The high values of specific strength and modulus of many filamentary materials have motivated substantial effort to utilize them in aerospace structures to save weight. Notable examples of such utilization are prevalent where surfaces of revolution are produced by filament winding techniques. The spectrum of applications has been extended since filaments imbedded in resinous matrices have become available in tape or sheet form. Limited utilization of such material in aircraft structural components has recently appeared wherein conventional metal structures have been replaced by filamentary composites. Substantial extension of this approach could eventually result in an especially efficient structure consisting primarily of filamentary composites. An extensive revision of existing fabrication methods would be required by the drastic changes inherent in the all-composite structure.

A design concept which could be utilized during the development period of the all-composite structure is that of enhancing conventionally designed metallic structures with resin-bonded filaments. This concept has considerable practical merit, since it retains the large background of technology developed for metal aircraft. For example, considerable weight saving is indicated if the longitudinal elements of monocoque structures are surface-reinforced with axially alined filaments. The axially loaded filaments are utilized efficiently and minimum amounts of the filamentary material are required. Shear stresses and inplane direct stresses are supported by the metal structure.

The purpose of this paper is to report the results of an exploratory research program conducted to determine the potential for weight saving offered by conventional metals reinforced on the surface with resin-bonded filaments. The program involved a series of filament-reinforced tubular compression specimens designed to indicate feasibility and to provide the strength and stiffness values necessary to demonstrate the weight-saving potential of filament-reinforced metals. The compressively loaded tube was selected for study because it lends itself conveniently to filamentary reinforcement and laboratory testing. In addition, tube columns are attractive because of the relatively simple and well developed analytical expressions for load-carrying capacity and structural efficiency.

SYMBOLS

The units used for physical quantities defined in this paper are given in both the U.S. Customary Units and in the International System of Units (SI) (ref. 1). Conversion factors pertinent to the present investigation are presented in appendix A.

D_m	mean diameter, inches (meters)
E	modulus of elasticity, pounds force/inch^2 (newtons/meter^2)
E_1	initial modulus of elasticity, pounds force/inch^2 (newtons/meter^2)
E_2	secondary modulus of elasticity, pounds force/inch^2 (newtons/meter^2)
E_c, E_f, E_m, E_r	modulus of elasticity of composite, filament, metal, and resin, respectively, pounds force/inch^2 (newtons/meter^2)
k	ratio of filament volume to volume of filament plus resin
L	length between end disks, inches (meters)

m mass, pounds mass (kilograms)

P compressive load, pounds force (newtons)

t total wall thickness of composite reinforced tube, inches (meters)

V volume fraction, ratio of constituent volume to total volume of reinforced metal tube (with subscript denoting the constituent)

$\alpha_c, \alpha_f, \alpha_m, \alpha_r$ coefficient of linear expansion of composite, filament, metal, and resin, respectively, per ^{o}F (per ^{o}K)

ϵ average axial strain

$\epsilon_c{}^R, \epsilon_m{}^R$ residual strain of composite and metal, respectively

ϵ_{max} average axial strain at failure

ρ density, pounds mass/foot^3 (kilograms/meter^3)

σ compressive stress, pounds force/inch^2 (newtons/meter^2)

$\sigma_c{}^R, \sigma_f{}^R, \sigma_m{}^R, \sigma_r{}^R$ residual stress of composite, filament, metal, and resin, respectively, pounds force/inch^2 (newtons/meter^2)

σ_f apparent filament stress at failure, $E_f\epsilon_{max}$, pounds force/inch^2 (newtons/meter^2)

$\bar{\sigma}_{max}$ average stress at maximum load, pounds force/inch^2 (newtons/meter^2)

σ_y compressive yield stress, pounds force/inch^2 (newtons/meter^2)

Subscripts:

Al aluminum

Mg magnesium

Ti titanium

TEST SPECIMENS

The test specimens consisted of metal tubing reinforced on the outer surface with unidirectional filaments bonded with epoxy resin and alined in the direction of the axis of the tubing. The shortest specimens (see fig. 1) were approximately 3 inches (7.6 cm) in length and were designed to obtain the maximum material compressive strength by crushing failure. The remainder of the specimens were designed to fail as columns and varied in length up to 30 inches (76 cm). The test program included 24 crushing specimens and 44 column specimens. The aluminum, titanium, and magnesium alloys designated in table I were included. Table I also lists the outside diameter and wall thickness of the metal tubing and the surface treatment used to prepare the tubing for bonding. The three types of tubing were axially reinforced with boron or S-glass filaments bonded with epoxy resin. The boron/epoxy material was obtained from an industrial processor in sheet form with nominally 220 filaments per inch (87 filaments per cm) of width of sheet. The boron filaments were 0.004 inch (0.10 mm) in diameter and impregnated with epoxy resin of the type listed in table II. Details of the S-glass/epoxy material used are also shown in table II.

The surface of the tubing was built up with individual layers such that the volume of composite material (filament/resin) was approximately equal to the volume of metal tubing. The layers consisted of individual plies of the number shown in table III, each having a longitudinal joint. The joints were staggered at equal intervals around the circumference of the tube. The tubing with layered reinforcement was enclosed in a close-fitting, heat-shrinkable plastic sleeve which, with mild heating, compacted the plies and squeezed out the entrapped air or gases. The specimens were then subjected to the cure cycles given in table II. More complete information on the fabrication process is given in reference 2.

The uniformity of the cross sections of the test specimens is indicated by the photomicrographs shown in figure 2. Figure 2(a) shows a portion of the wall of a titanium tube reinforced with five layers of boron/epoxy. Figure 2(b) shows three plies of the S-glass/epoxy on a portion of the wall of an aluminum tube. The irregular shapes shown in the composite portion of figure 2(b) are resin-rich areas. The volume fractions of the constituents as obtained from a sample of each type of specimen are given in table III. The volume of metal and the total volume were determined from the dimensions of the tubing before and after reinforcement. The volume of boron filament was determined from the dimensions and the number of filaments counted on a photomicrograph of a typical cross section of each type of boron-reinforced tubing. The volume of S-glass filament was determined by the resin burnout technique described in reference 3. Inspection of photomicrographs of cross sections of the specimens indicated that the quality of the fabrication process was such that the specimens were essentially free of voids.

The ends of the specimens were mounted in hardened steel disks (see fig. 1) of 1-inch (2.5-cm) diameter and 0.25-inch (0.63-cm) thickness. One side of each disk contained a concentric circular recess 0.125 inch (0.32 cm) in depth and of width sufficient to accommodate one end of the specimen and additional epoxy resin. This mounting supported the specimen in such a manner as to prevent separation of the filament ends.

METHOD OF TESTING

A typical compressive specimen for crushing failure is shown in the testing machine in figure 3 and a typical column specimen is shown in figure 4. The testing-machine platens were alined parallel to the disks on the ends of the specimen in order to approach uniform compressive loading in the axial direction on the specimen ends. The loading was increased at a uniform strain rate of 0.001 per minute until failure of the specimen. Two foil-type resistance strain gages mounted diametrically opposite on the outer surface and midway along the length of each specimen provided axial strain data. The data were recorded in the Langley central digital data recording facility and were monitored during the tests on an oscilloscope.

EXPERIMENTAL RESULTS

The test specimens were all subjected to axial compression but were designed for two distinct types of behavior, namely, crushing tests in which the specimens remained straight until failure, and column tests in which the specimens failed by column instability. The following experimental results are separated accordingly.

Crushing Tests

Typical compressive stress-strain curves for magnesium, aluminum, and titanium tubes reinforced with S-glass/epoxy or boron/epoxy are shown in figure 5. The results were obtained from the specimens of shortest length. The stresses were based on the total cross-sectional area of the metal tubing and composite reinforcement, and the strains were obtained from the average of the two diametrically opposite longitudinal strains measured on the outer surface at midlength of the specimens. For comparison, stress-strain curves for metal tubing without reinforcement were obtained experimentally and are presented by dashed curves. Prior to testing, the metal tubing had been subjected to the same temperature-time conditions as prescribed by the cure cycle in table II for the corresponding reinforced metal specimens.

The stress-strain curves for the reinforced metals shown in figure 5 consist of two straight lines. The modulus or slope of the initial straight line E_1 closely correlates

with the calculated values obtained from the rule of mixtures and prescribes the stress-strain behavior until the unit shortening is such that the metal component is strained plastically. The curves clearly indicate that the strain at the elastic limit of the metal component differs from that for the knee of the stress-strain curve for the reinforced metal. The deviation varies for the various metal-filament combinations investigated. The phenomenon is believed to be associated with a residual strain introduced during the curing process of the reinforced metal tubes and is treated more fully in the section entitled "Discussion." Above the knee the stress-strain relationship is also a straight line but at a lower value of slope or tangent modulus E_2 which is essentially of the magnitude prescribed by the stiffness of the filamentary reinforcement alone. The values of E_1 and E_2 obtained experimentally for each of the crushing specimens are given in table IV. The average stress at maximum load $\bar{\sigma}_{max}$, the corresponding strain ϵ_{max}, and the apparent maximum filament stress σ_f obtained from the product of the filament modulus and ϵ_{max} are also listed in table IV for each specimen. Note that apparent compressive stresses σ_f for boron filament of 600 ksi (4100 MN/m^2) and over are indicated with one exception. Somewhat higher stresses in the filaments are indicated when the residual stresses are considered (see "Discussion" section). The average values of the various properties are included in the table for each group of specimens.

Typical failures of the crushing specimens are shown in figure 6. Failures occurred abruptly with no prior warning indicated audibly, visually, or by the load or strain indicators. Inspection of the failed specimens showed the composite material well splintered with debonding at the metal-resin interface as the composite separated and exposed a clean metal surface without attached resin particles. In several cases a circumferential buckle developed in the metal tubing probably after failure of the composite. In all cases the failure occurred beyond the yield strain of the metal as indicated by the values of ϵ_{max} listed in table IV.

Some evidence that the debonding at failure may be coincident with failure in the reinforcing material is provided by data obtained in conjunction with the tests reported in reference 2 for similar tubing but without the metal component. The average strain at failure for the boron/epoxy and the glass/epoxy specimens of reference 2 was found to be 1.1 percent and 2.7 percent, respectively. These values are remarkably consistent with the values listed in table IV for the metals reinforced with these composites. This consistency of the axial deformation at failure suggests that failure of the composite reinforced metal may be a direct consequence of a local failure initiated in the composite component.

Column Tests

Typical stress-strain behavior for the column specimens is shown in figure 7. The initial portion of the stress-strain curve, like that for the crushing specimens, is a straight line of slope or modulus closely in conformance with that calculated with the rule of mixtures. Column bending is indicated by the deviation of the outer surface axial strains on opposite sides of the column as shown by the separating of the curves at the upper portion of figures 7(a) and 7(b). Stress-strain behavior due to column bending of the type indicated in figure 7(a) occurs when the stresses are elastic, while figure 7(b) shows the behavior when stresses in the metal tubing are well in the plastic range. The knee in the initial straight line shown in figure 7(b) occurs when the deformation of the composite is such that the metal component is strained plastically as in the case of the crushing specimens.

The average stress at maximum load of the column specimens $\bar{\sigma}_{max}$ is listed in table V along with values of the length-to-mean diameter ratio L/D_m of the various types of boron-reinforced metal tubing. The total wall thickness and length of specimen between end disks are also given in table V. Similar test results and dimensions for the glass-reinforced metal tubing are given in table VI.

A typical instability failure of a long column specimen is shown in figure 8. The clamped-end mode of instability occurred in all the columns; however, at buckling, the shorter columns developed sudden debonding, filament splintering, and breaking failures.

EXPERIMENTAL AND ANALYTICAL COMPARISONS

The values of average stress at maximum load for the crushing and column specimens of the various reinforced metals are plotted for values of L/D_m in figure 9. Also shown in figure 9 are curves as given by the Euler equation for a tubular column with clamped-end conditions. The lower Euler curve shown in each part of the figure was obtained by using the average values of E_1 from table IV for the crushing specimens of the various reinforced metals. Similarly, the upper curve in each part of the figure was obtained by using the appropriate average value of E_2 from table IV. The dashed line shown connecting the two curves is at the average stress level for which the stress-strain slope changed from E_1 to E_2 for the crushing specimens. The column data show good correlation with the curves and indicate that close to clamped-end conditions were obtained in the experiments.

The reinforced metals are compared with similar commonly used metal alloys on a mass-strength basis in figure 10 where the mass parameter m/L^3 is shown for values of the column structural index P/L^2. The results shown in figure 10 are not for the

most "efficient" columns (as defined in ref. 4) but for specific values of D_m/t corresponding to the columns that were tested. The data points show the values as obtained from the tests reported herein and the curves show calculated results. The lower parts of the curves are the values given by the Euler equation for a tubular column with clamped ends. This equation may be expressed in terms of the mass parameter and structural index as

$$\frac{m}{L^3} = \left(\frac{P/L^2}{\frac{\pi}{2} \frac{E}{\rho^2} \frac{D_m}{t}} \right)^{1/2} \tag{1}$$

For the reinforced metals, the two values of moduli E_1 and E_2 as previously described for figure 5 are introduced for E. The use of these values results in the straight lines joined by the dashed lines in the lower parts of the curves in figure 10. The dashed lines, as previously explained for figure 9, are the average stress levels at which the slope changes from E_1 to E_2 for the crushing specimens.

The upper parts of the curves in figure 10 were obtained from the compressive strength of the metals and the reinforced metals and may be expressed by

$$\frac{m}{L^3} = \frac{\rho}{\bar{\sigma}_{max}} \frac{P}{L^2} \tag{2}$$

In this equation the compressive yield stresses were used for the values of $\bar{\sigma}_{max}$ for the metals and the average values of $\bar{\sigma}_{max}$ given in table IV were used for the reinforced metals.

The mass-strength comparisons in figure 10 show a substantial improvement in the efficiency of metals when reinforced with the boron/epoxy composite for the various values of D_m/t indicated. The S-glass/epoxy reinforcement also substantially improves the efficiency of the aluminum or magnesium when these metals are stressed into the plastic range (high values of P/L^2). In the elastic range (low values of P/L^2), the glass reinforcement provides some improvement in efficiency of the aluminum but slightly decreases the efficiency of the magnesium.

DISCUSSION

The compressive properties shown for metals reinforced with resin-bonded filaments in figure 5 and table IV are remarkable when compared with the properties of the basic metals. Material such as aluminum-boron/epoxy with a density 15 percent less →

than aluminum alloy, a compressive strength over 200 ksi (1380 MN/m^2), and a modulus of elasticity of 22 500 ksi (155 GN/m^2) should merit considerable attention in the design of structures. Similar results are indicated by the other metals and reinforcements shown in figure 5 and table IV. An example of the benefits provided by utilizing the stiffness properties of titanium reinforced with boron/epoxy for aircraft floor beams recently has been demonstrated in reference 5.

A basic difference of the filamentary reinforced metal from the metal alone is the shape of the stress-strain curves. The reinforced-metal stress-strain curves shown in figure 5 do not display the plastic range characteristic of the metal alloys commonly used in aerospace structures. The structures therefore may be expected to have somewhat brittle characteristics. The stress-strain curves for the metals reinforced with boron/epoxy exhibit only a slight reduction in modulus at high stresses and the behavior remains linear although the strains are well into the plastic range of the metals. In addition, the strain at failure for the boron/epoxy-reinforced metals as listed in table IV is only about 1 percent. Additional test specimens not reported herein were unloaded after being subjected to strains beyond the knee in the curve, and the return stress-strain relationship was linear with a permanent offset from zero similar to that characteristic of metals. Increasing the ratios of boron filament to metal to values greater than 1/2 would be expected to make the material more brittle-like in behavior, while lower ratios would likely lead to characteristics approaching the stress-strain behavior of the metal. The metals reinforced with glass/epoxy failed at values of ϵ_{max} from 2.5 to 3.1 percent, considerably greater than the values for the boron/epoxy-reinforced metals. The strain range beyond the knee until failure is also much greater for the tubes reinforced with glass/epoxy than for those reinforced with boron/epoxy. In addition, unloading from strains in this range should result in considerably greater permanent deformations than occur for the boron/epoxy-reinforced metals.

The location of the knee in the stress-strain curve of the reinforced metals occurs when the metal component changes from elastic to plastic behavior. In order to evaluate this transition it is necessary to consider the residual strain in the metal component which is introduced upon cooling from the curing temperature. For the reinforced metals reported herein, residual tension is developed in the metals and is equilibrated by compression in the composites (boron/epoxy or S-glass/epoxy). The initial external compressive loading of the reinforced metals relieves the residual state of tension of the metal component. Further compressive loading introduces compression into the metal component with linear stress-strain behavior until the compressive elastic limit is exceeded. The strain at the knee in the stress-strain curves for the reinforced metals as shown in figure 5 is thus offset from the elastic-limit strain of the metal by an amount equal to the residual strain in the metal component. The residual stresses and strains

in the reinforced metals were evaluated from elementary thermal stress theory (see, for example, ref. 6) for a bar consisting of two materials with different expansion and extensional stiffness properties. The composite (filament/resin) was treated as one material and the metal as the other. The longitudinal modulus of elasticity for the composites E_c was evaluated by the rule of mixtures. Similarly, the longitudinal expansion coefficient for the composite α_c (see ref. 7) was obtained from

$$\alpha_c E_c = kE_f\alpha_f + (1 - k)E_r\alpha_r \tag{3}$$

The constants employed in the calculations are given in table VII, and the resulting strains and stresses for the various constituents of each of the reinforced metals are presented in table VIII. The values of residual strain for the metal components were superposed to the elastic limit strain of the metals in figure 5 to indicate the agreement with the knee of the curve for the reinforced metals.

Cyclic load and fatigue problems may be especially important beyond the knee in the stress-strain curve since the metal component is operating plastically in this range. The knee in the curve, then, might be viewed in the same light as the yield of conventional metals and could be of particular importance in applications designed for continuous or longtime service. Inspection of figure 5 shows that the limitations would be especially severe for the S-glass/epoxy-reinforced metals since the knee occurs early in the stress-strain history. The titanium-boron/epoxy would be least penalized of the materials shown since the knee in the stress-strain curve occurs nearest to failure.

Material comparisons of the various reinforced metals with titanium are shown in figure 11, and the material properties used in the comparisons are listed in table IX. Also included are results for two all-composite materials, boron/epoxy and S-glass/epoxy, obtained from data presented in reference 2. These all-composite materials were fabricated by using the same preimpregnated filamentary material and cure cycle listed in table II and resulted in relative volume fractions similar to those listed in table III. The parameter $\rho/E_1^{1/2}$ shown in figure 11(a) may be identified from equation (1) which applies to column-buckling failure and excludes other modes of failure. This parameter is normalized with respect to the parameter for titanium $\left(\frac{\rho}{E^{1/2}}\right)_{\text{Ti-6Al-4V}}$. Inspection of figure 11(a) shows that all the reinforced metals are substantially lighter as columns than titanium. Boron/epoxy-reinforced magnesium columns are less than 40 percent of the weight of titanium columns, and the same reinforcement on aluminum performs almost as efficiently. Boron/epoxy columns are about 32 percent of the weight of the titanium column, and S-glass/epoxy columns weigh about 62 percent of the titanium column.

In figure 11(b) the materials are compared on the basis of compressive strength by using the mass-strength parameter ρ/σ normalized with respect to the parameter for

titanium $\left(\frac{\rho}{\sigma_y}\right)_{\text{Ti-6Al-4V}}$. Two values are shown for the reinforced metals; the lower values indicated by the dashed lines result when σ is the stress at failure, while the upper values correspond to σ equal to the stress at the knee in the stress-strain curve. On the basis of yield strength or the knee in the stress-strain curve, the glass/epoxy-reinforced metals are not competitive but the boron/epoxy-reinforced metals are about one-half the weight of titanium. On the basis of maximum strength, all the reinforced metals as shown by the dashed lines are less than one-half the weight of titanium and the boron/epoxy-reinforced magnesium is only about one-fourth as heavy as the titanium. The boron/epoxy composite weighs only 18 percent the weight of titanium, and the S-glass/epoxy composite weighs about 26 percent the weight of titanium.

Figure 11 shows that the all-composite materials are more efficient than the reinforced metals. At the present time, however, the lack of advanced fabrication and joining technology deters the use of all-composite materials on a large-scale basis. The reinforced-metal materials could substantially utilize existing fabrication technology and thereby offer a significant advantage over all-composite materials for aircraft structural applications in the immediate future.

CONCLUDING REMARKS

The feasibility of surface reinforcing metals with resin-bonded filamentary materials has been demonstrated for aluminum, magnesium, and titanium alloy tubing reinforced with boron or S-glass filaments. Compression tests of specimens consisting, by volume, of approximately 50 percent metal, 25 percent boron filament, and 25 percent resin showed remarkable mechanical properties indicating substantial weight-saving potential for aerospace structures. Mass-strength comparisons showed the boron-reinforced metals to weigh from 25 to 40 percent of the weight of titanium for compressive crushing strength and from 40 to 60 percent for column instability. Magnesium or aluminum reinforced with S-glass filaments weighs less than 50 percent of titanium for compressive crushing and about 70 percent for column instability.

The reinforcement of metals with bonded filaments is a concept which utilizes high-performance filaments in conjunction with the well developed background of fabrication technology for aerospace structures. This advantage along with the weight-saving potential indicated herein suggests important practical application in structural design.

Langley Research Center,
National Aeronautics and Space Administration,
Langley Station, Hampton, Va., August 20, 1968,
124-08-01-10-23.

APPENDIX A

CONVERSION OF U.S. CUSTOMARY UNITS TO SI UNITS

The International System of Units (SI) was adopted by the Eleventh General Conference on Weights and Measures, Paris, October 1960 (ref. 1). Conversion factors for the units used herein are given in the following table:

Physical quantity	U.S. Customary Unit	Conversion factor (*)	SI Unit
Length	in.	0.0254	meters (m)
Temperature . .	(^{o}F + 460)	5/9	degrees Kelvin (^{o}K)
Density	lbm/in^3	27.68×10^3	kilograms per cubic meter (kg/m^3)
Load	lbf	4.448	newtons (N)
Mass	lbm	0.4536	kilograms (kg)
Modulus, stress .	psi = lbf/in^2	6895	newtons per square meter (N/m^2)

*Multiply value given in U.S. Customary Units by conversion factor to obtain equivalent value in SI Unit.

Prefixes to indicate multiple of units are as follows:

Prefix	Multiple
centi (c)	10^{-2}
kilo (k)	10^3
mega (M)	10^6
giga (G)	10^9

REFERENCES

1. Comm. on Metric Pract.: ASTM Metric Practice Guide. NBS Handbook 102, U.S. Dep. Com., Mar. 10, 1967.

2. Davis, John G., Jr.: Fabrication of Uniaxial Filament-Reinforced Epoxy Tubes for Structural Applications. Paper to be presented at 14th National SAMPE Symposium, (Cocoa Beach, Fla.), Nov. 5-7, 1968.

3. Davis, John G., Jr.; and Zender, George W.: Compressive Behavior of Plates Fabricated From Glass Filaments and Epoxy Resin. NASA TN D-3918, 1967.

4. Shanley, F. R.: Weight-Strength Analysis of Aircraft Structures. Dover Publ., Inc., c.1960.

5. Lager, John R.; and June, Reid R.: Design, Analysis, Fabrication and Test of a Boron Composite Beam. J. Compos. Mater., vol. II, no. 2, Apr. 1968, pp. 128-137.

6. Timoshenko, S.: Strength of Materials. Part I – Elementary Theory and Problems. D. Van Nostrand Co., Inc., 1930, pp. 25-27.

7. Greszczuk, Longin B.: Thermoelastic Considerations for Filamentary Structures. Proceedings 20th Anniversary Technical Conference, sec. 5-C, Soc. Plast. Ind., Inc., Feb. 1965.

TABLE I.- DETAILS OF METAL TUBING

Metal tubing	Tubing dimensions				Surface preparation for bonding
	Outside diameter		Wall thickness		
	in.	cm	in.	cm	
6061-T6 aluminum alloy	0.500	1.270	0.022	0.056	Chemically cleaned with chromic-sulfuric acid solution
Ti-6Al-4V titanium alloy	.507	1.288	.032	.081	Blast with 220-grit aluminum oxide followed by Pasa-Jell[a] treatment.
AZ31B-F magnesium alloy	.500	1.270	.035	.089	Chemically cleaned with chromic-nitric acid solution

[a]Semco Sales & Service, Inc.

TABLE II.- DETAILS OF PREIMPREGNATED SHEET OR TAPE AND CURING CONDITIONS

Filament	Designation of resin system or preimpregnated tape	Resin content, percent by weight	Backing	Nominal thickness per ply	Exposure conditions for resin cure of reinforced tubing
Boron[a]	1031/828/MNA/BDMA[b]	29 ± 3	104 glass scrim cloth	0.005 to 0.006 in. (0.13 to 0.15 mm)	1 hour at 180° F (355° K) plus 3 hours at 350° F (450° K)
S-glass	XP-251S[c]	25 ± 3	None	0.0075 in. (0.19 mm)	12 hours at 300° F (422° K)

[a]Texaco Experiment Incorporated.

[b]Shell Chemical Company.

[c]Minnesota Mining & Manufacturing Company.

TABLE III.- CONSTITUENT VOLUME FRACTIONS AND NUMBER OF PLIES

Material	Constituent volume / Total volume			Number of plies
	Metal	Filament	Resin	
Aluminum-boron/epoxy	0.47	0.27	0.26	4
Titanium-boron/epoxy	.52	.25	.23	5
Magnesium-boron/epoxy	.49	.26	.25	6
Aluminum—S-glass/epoxy	.47	.32	.21	3
Magnesium—S-glass/epoxy	.48	.31	.21	4

TABLE IV.- RESULTS FOR CRUSHING SPECIMENS

Material and length	t		Tangent modulus				$\bar{\sigma}_{max}$		ϵ_{max}, percent	σ_f	
			E_1		E_2						
	in.	cm	ksi	GN/m^2	ksi	GN/m^2	ksi	MN/m^2		ksi	MN/m^2
Aluminum-	0.044	0.112	22 600	156	18 600	128	189	1300	0.9	540	3700
boron/epoxy;	.044	.112	-----	---	-----	---	208	1430	--	---	----
L = 2.8 in.	.045	.114	22 200	153	18 300	126	213	1470	1.1	660	4600
(7.1 cm)	.045	.114	22 700	156	18 500	128	200	1380	1.0	600	4100
Averages	0.044	0.112	22 500	155	18 500	128	202	1390	1.0	600	4100
Titanium-	0.059	0.150	24 000	166	16 000	110	223	1540	1.0	600	4100
boron/epoxy;	.059	.150	24 000	166	16 000	110	233	1610	1.0	600	4100
L = 2.8 in.	.059	.150	23 800	164	15 800	109	236	1630	1.1	660	4600
(7.1 cm)	.059	.150	24 000	166	15 600	108	226	1560	1.0	600	4100
	.060	.152	23 900	165	15 100	104	222	1530	1.0	600	4100
Averages	0.059	0.150	23 900	165	15 700	108	228	1570	1.0	600	4100
Magnesium-	0.069	0.175	18 800	130	16 700	115	185	1280	1.1	660	4600
boron/epoxy;	.068	.173	19 000	131	16 800	116	182	1260	1.0	600	4100
L = 3.0 in.	.068	.173	18 900	130	-----	---	178	1230	--	---	----
(7.6 cm)	.068	.173	19 000	131	16 800	116	199	1370	1.1	660	4600
	.068	.173	18 800	130	17 000	117	203	1400	1.1	660	4600
Averages	0.068	0.173	18 900	130	16 800	116	189	1300	1.1	660	4600
Aluminum—	0.046	0.117	-----	---	-----	---	140	960	--	---	----
S-glass/epoxy;	.046	.117	8 800	61	4 400	30	129	890	2.5	310	2200
L = 2.8 in.	.046	.117	8 800	61	4 400	30	135	930	2.6	320	2200
(7.1 cm)	.046	.117	8 700	60	4 400	30	133	920	2.6	320	2200
	.046	.117	8 800	61	4 400	30	138	950	2.7	340	2300
Averages	0.046	0.117	8 800	61	4 400	30	135	930	2.6	320	2200
Magnesium—	0.070	0.178	6 500	45	4 000	28	120	830	2.7	340	2300
S-glass/epoxy;	.069	.175	6 500	45	3 800	26	129	890	2.8	350	2400
L = 3.0 in.	.069	.175	6 400	44	3 700	26	119	820	3.0	380	2600
(7.6 cm)	.070	.178	6 500	45	3 800	26	109	750	2.7	340	2300
	.069	.175	6 400	44	3 800	26	128	880	3.1	390	2700
Averages	0.069	0.175	6 500	45	3 800	26	121	830	2.9	360	2500

TABLE V.- RESULTS FOR COLUMN SPECIMENS WITH BORON/EPOXY REINFORCEMENT

Material	t		L		L/D_m	$\bar{\sigma}_{max}$	
	in.	cm	in.	cm		ksi	MN/m^2
Aluminum-boron/epoxy	0.046	0.117	9.90	25.15	19.72	174	1200
	.045	.114	9.91	25.17	19.78	162	1120
	.046	.117	11.38	28.91	22.67	135	930
	.046	.117	11.49	29.18	22.89	133	920
	.045	.114	14.98	38.05	29.90	106	730
	.046	.117	15.09	38.33	30.06	103	710
	.046	.117	19.92	50.60	39.68	64	440
	.045	.114	19.97	50.72	39.86	66	460
	.046	.117	30.00	76.20	59.76	29	200
	.046	.117	30.03	76.28	59.82	29	200
Titanium-boron/epoxy	.058	.147	8.75	22.22	17.46	217	1500
	.058	.147	9.27	23.55	18.50	207	1430
	.059	.150	14.51	36.86	28.90	127	880
	.060	.152	15.01	38.12	29.84	115	790
	.060	.152	19.72	50.09	39.20	72	500
	.060	.152	19.72	50.09	39.20	71	490
	.060	.152	30.00	76.20	59.64	32	220
	.060	.152	30.00	76.20	59.64	32	220
Magnesium-boron/epoxy	.063	.160	9.50	24.13	19.31	136	940
	.070	.178	9.50	24.13	19.04	155	1070
	.063	.160	14.50	36.83	29.47	91	630
	.068	.173	15.02	38.15	30.22	84	580
	.068	.173	19.75	50.16	39.74	57	390
	.067	.170	19.75	50.16	39.82	60	410
	.067	.170	30.00	76.20	60.48	26	180
	.068	.173	30.00	76.20	60.36	26	180

TABLE VI.- RESULTS FOR COLUMN SPECIMENS

WITH S-GLASS/EPOXY REINFORCEMENT

Material	t		L		L/D_m	$\bar{\sigma}_{max}$	
	in.	cm	in.	cm		ksi	MN/m^2
Aluminum—	0.046	0.117	7.80	19.81	15.54	93	640
S-glass/epoxy	.046	.117	7.81	19.84	15.56	90	620
	.046	.117	9.68	24.59	19.28	67	460
	.045	.114	9.70	24.64	19.36	65	450
	.046	.117	13.50	34.29	26.89	41	280
	.046	.117	13.50	34.29	26.89	42	290
	.046	.117	19.71	50.06	39.26	26	180
	.046	.117	19.75	50.16	39.34	27	190
	.047	.119	29.75	75.56	59.14	12	80
	.047	.119	29.77	75.62	59.18	12	80
Magnesium—	.064	.163	9.73	24.71	19.70	55	380
S-glass/epoxy	.065	.165	9.75	24.76	19.70	53	360
	.064	.163	14.68	37.29	29.72	28	190
	.065	.165	15.77	40.06	31.86	25	170
	.065	.165	19.75	50.16	39.90	19	130
	.066	.168	19.75	50.16	39.82	18	120
	.065	.165	29.67	75.36	59.94	9	60
	.066	.168	29.72	75.49	59.92	9	60

TABLE VII.- CONSTANTS FOR EVALUATION OF RESIDUAL STRESS AND STRAIN

Material	k	E_f		E_r		E_c		E_m		α_f		α_r		α_c		α_m		Temperature drop after curing	
		ksi	GN/m^2	ksi	GN/m^2	ksi	GN/m^2	ksi	GN/m^2	per ^oF	per ^oK	per ^oF	per ^oK	per ^oF	per ^oK	per ^oF	per ^oK	^oF	^oK
Aluminum-boron/epoxy	0.51	60 000	414	500	3.4	30 800	212	10 000	69	2.7×10^{-6}	4.9×10^{-6}	16.0×10^{-6}	28.8×10^{-6}	2.8×10^{-6}	5.0×10^{-6}	13.6×10^{-6}	24.5×10^{-6}	270	150
Titanium-boron/epoxy	.52	60 000	414	500	3.4	31 400	217	15 500	107	2.7	4.9	16.0	28.8	2.8	5.0	5.4	9.7	270	150
Magnesium-boron/epoxy	.51	60 000	414	500	3.4	30 800	212	6 500	45	2.7	4.9	16.0	28.8	2.8	5.0	14.5	26.1	270	150
Aluminum—S-glass/epoxy	.60	12 500	86	500	3.4	7 700	53	10 000	69	1.6	2.9	16.0	28.8	2.0	3.6	13.6	24.5	220	122
Magnesium—S-glass/epoxy	.60	12 500	86	500	3.4	7 700	53	6 500	45	1.6	2.9	16.0	28.8	2.0	3.6	14.5	26.1	220	122

TABLE VIII.- RESIDUAL STRESS AND STRAIN OF REINFORCED-METAL CONSTITUENTS

[Negative values indicate tension]

Material	ϵ_m^R	ϵ_c^R	σ_m^R		σ_c^R		σ_f^R		σ_r^R	
			ksi	MN/m^2	ksi	MN/m^2	ksi	MN/m^2	ksi	MN/m^2
Aluminum-boron/epoxy	-0.00227	0.00065	-22.70	-156.52	20.02	138.04	39.00	268.91	0.32	2.21
Titanium-boron/epoxy	-.00046	.00025	-7.13	-49.16	7.85	54.13	15.00	103.42	.12	.83
Magnesium-boron/epoxy	-.00263	.00053	-17.10	-117.90	16.32	112.53	31.80	219.26	.26	1.79
Aluminum—S-glass/epoxy	-.00119	.00137	-11.90	-82.05	10.55	72.74	17.12	118.04	.68	4.69
Magnesium—S-glass/epoxy	-.00149	.00127	-9.68	-66.74	9.78	67.44	15.88	109.49	.64	4.41

TABLE IX.- MATERIAL PROPERTIES

Material	ρ		E_1		σ_y		$\bar{\sigma}_{max}$	
	lbm/in^3	Mg/m^3	ksi	GN/m^2	ksi	MN/m^2	ksi	MN/m^2
6061-T6 aluminum	0.098	2.71	10 000	69	42	290	---	----
AZ31B-F magnesium	.064	1.77	6 500	45	13	90	---	----
Ti-6Al-4V	.160	4.43	15 500	107	125	860	---	----
Aluminum-boron/epoxy	.083	2.30	22 500	155	125	860	202	1390
Magnesium-boron/epoxy	.067	1.85	18 900	130	90	620	189	1300
Titanium-boron/epoxy	.117	3.24	23 900	165	200	1380	228	1570
Boron/epoxy	.072	1.99	30 000	207	---	----	310	2140
Aluminum—S-glass/epoxy	.084	2.32	8 800	61	45	310	139	930
Magnesium—S-glass/epoxy	.068	1.88	6 500	45	25	170	121	830
S-glass/epoxy	.071	1.96	8 000	55	---	----	210	1450

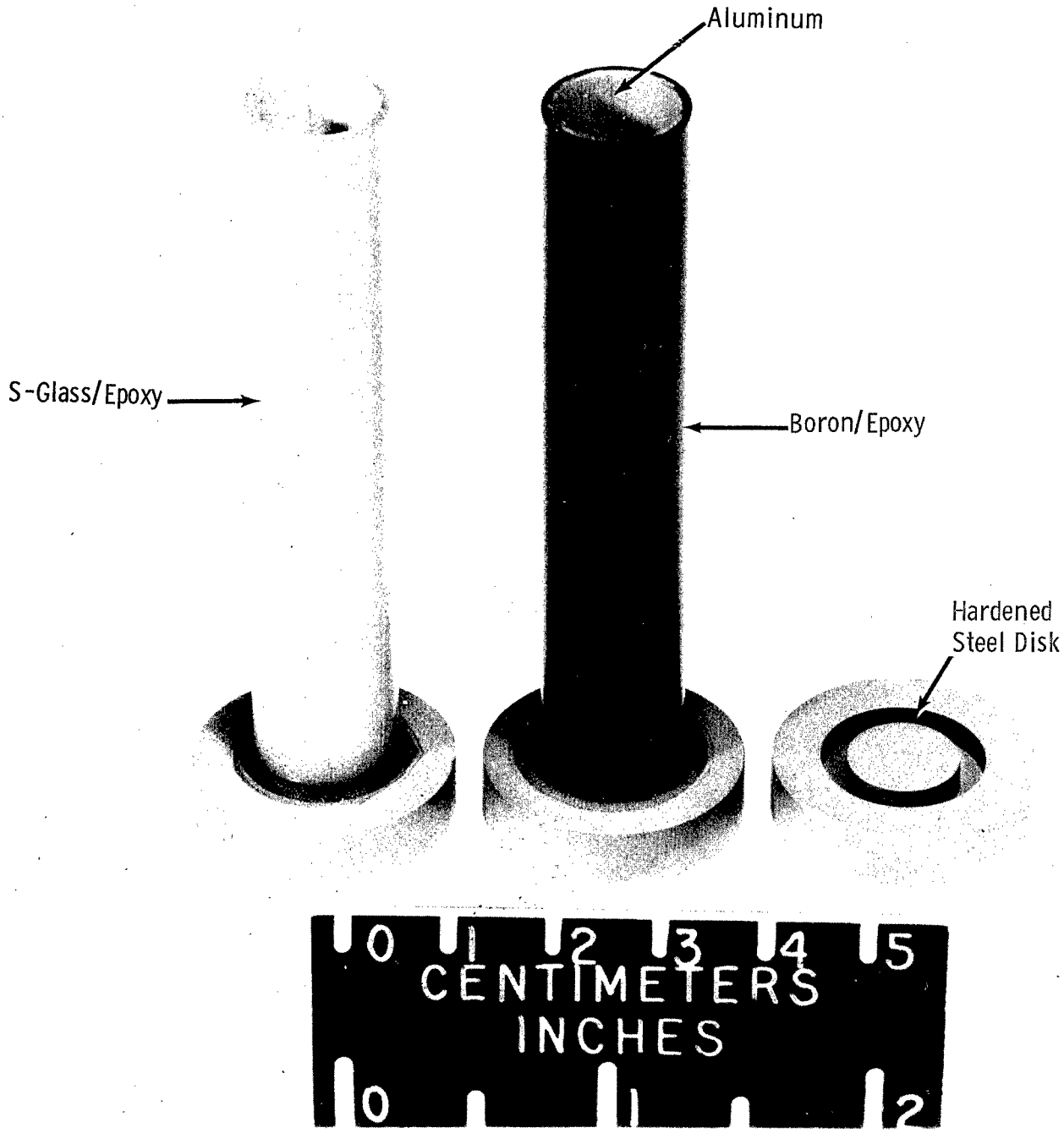

Figure 1.- Typical specimens designed for crushing failure. L-68-5695

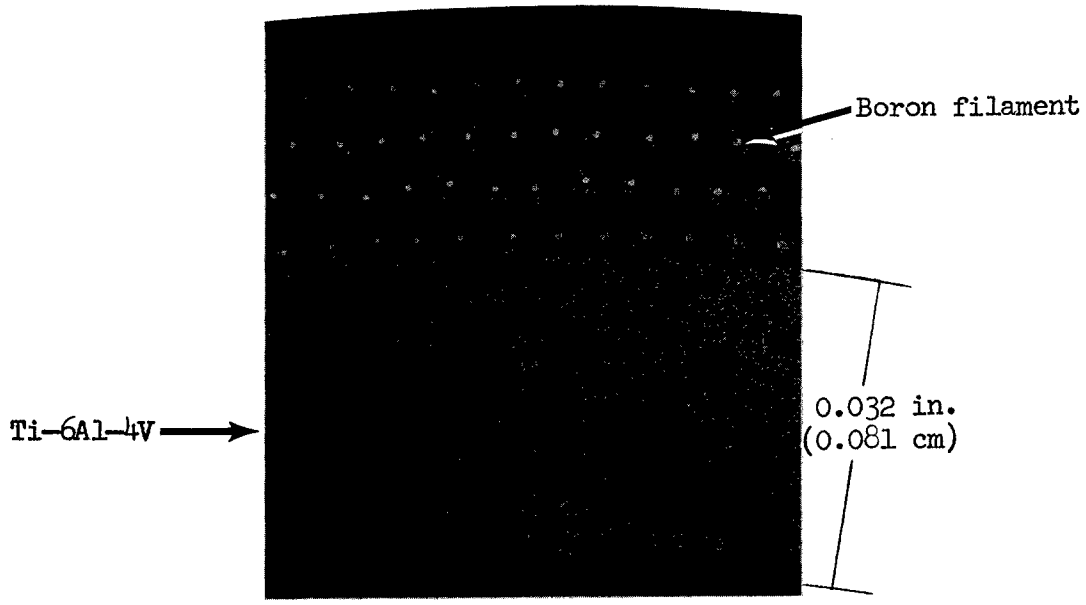

(a) Portion of titanium tube wall reinforced with boron/epoxy.

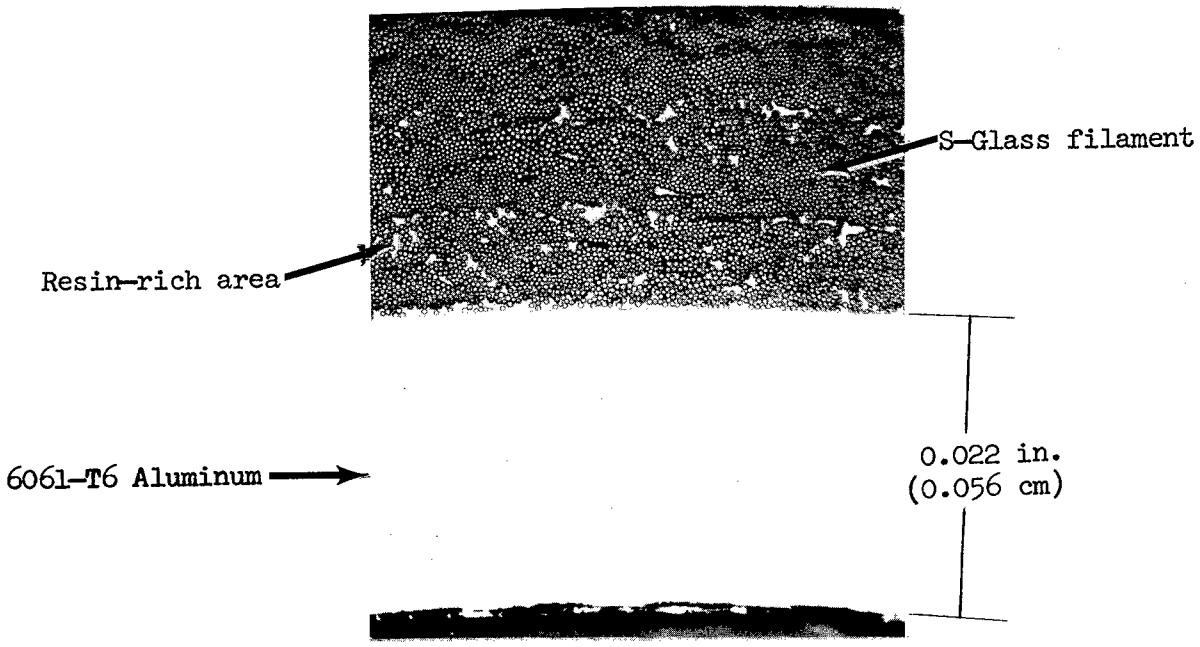

(b) Portion of aluminum tube wall reinforced with S-glass/epoxy.

L-68-5696

Figure 2.- Photomicrographs of typical specimen cross sections.

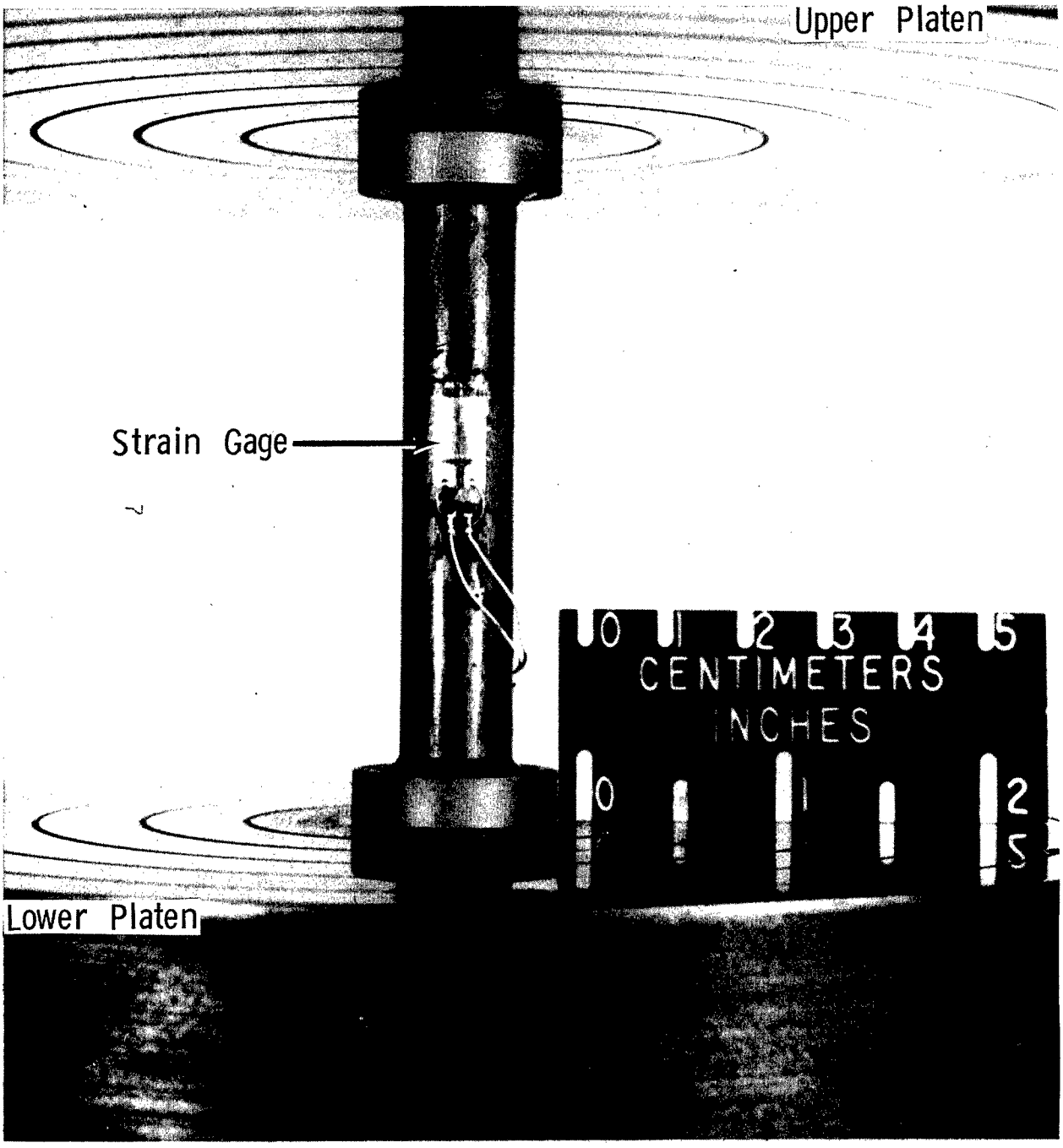

Figure 3.- Test apparatus for crushing test. L-68-5697

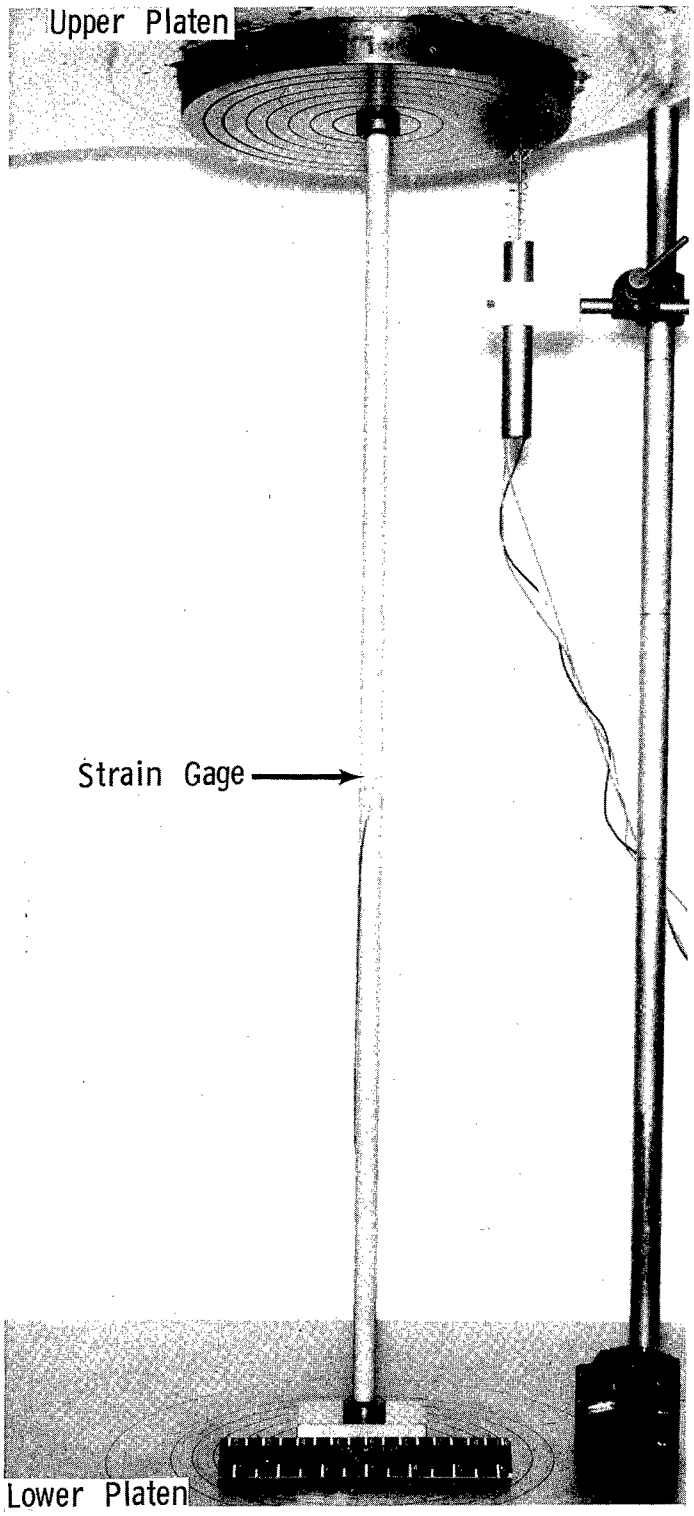

Figure 4.- Test apparatus for column test. L-68-5698

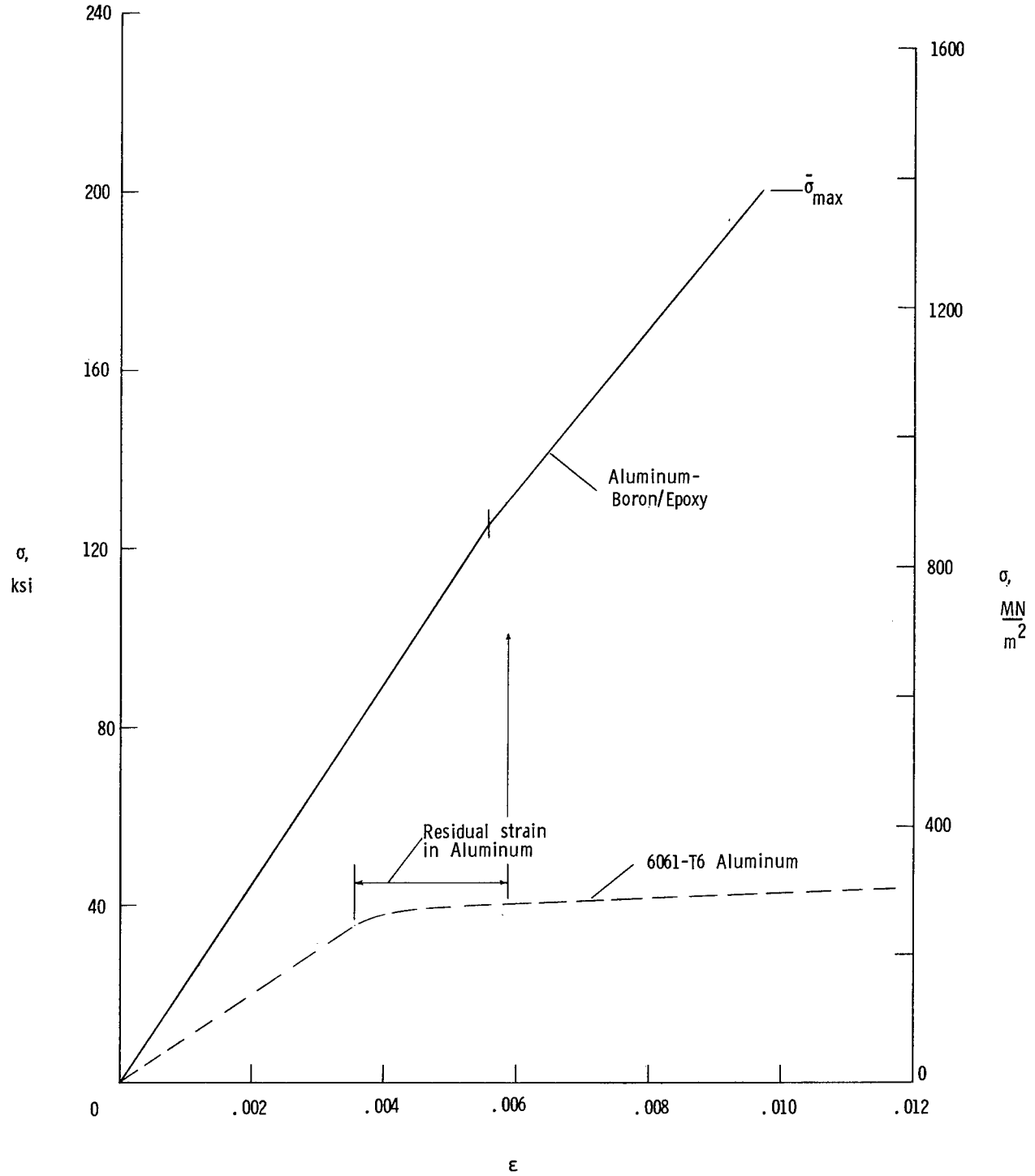

(a) Aluminum and aluminum-boron/epoxy.

Figure 5.- Compressive stress-strain curves for metal tubing and filamentary reinforced metal tubing.

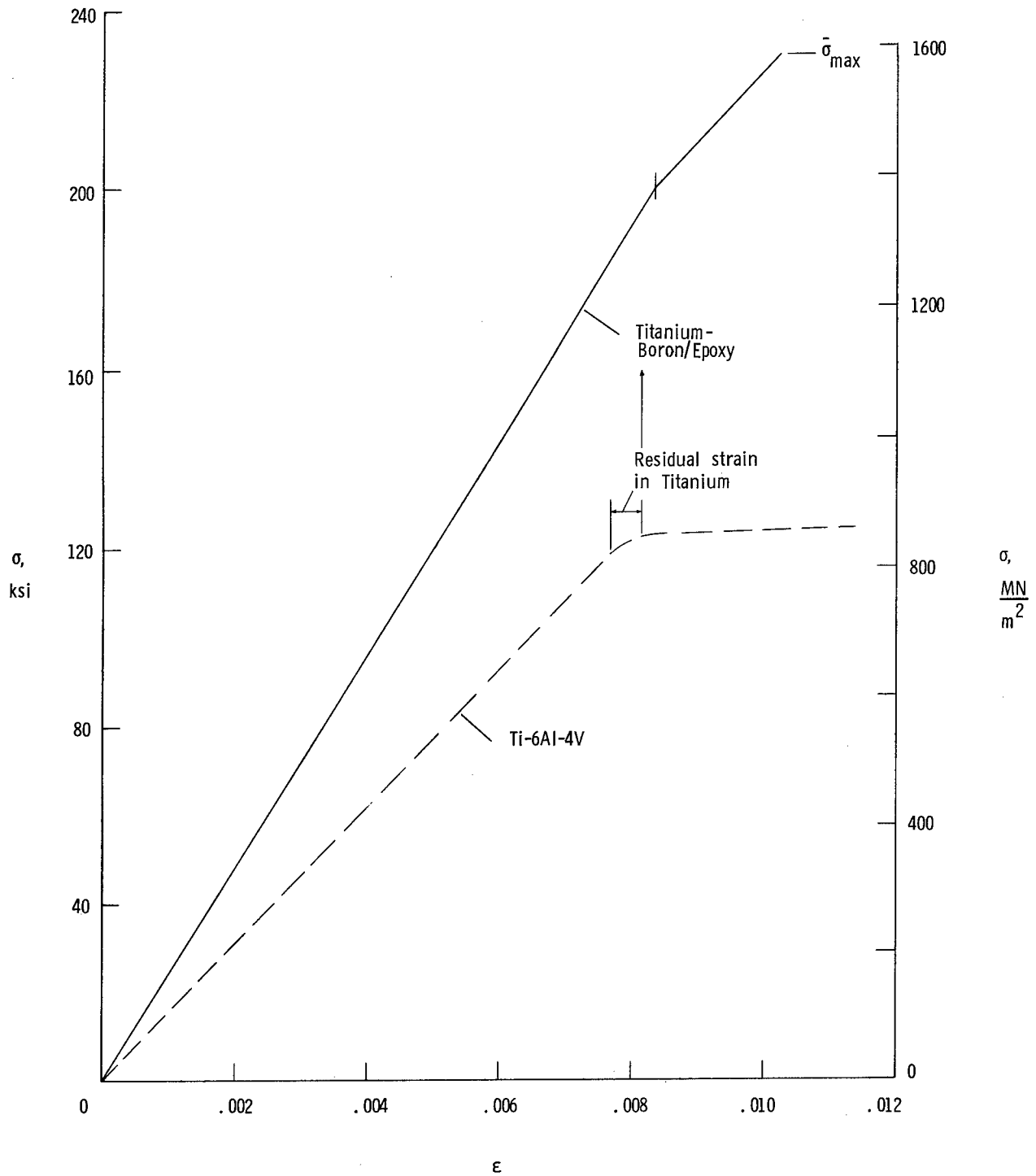

(b) Titanium and titanium-boron/epoxy.

Figure 5.- Continued.

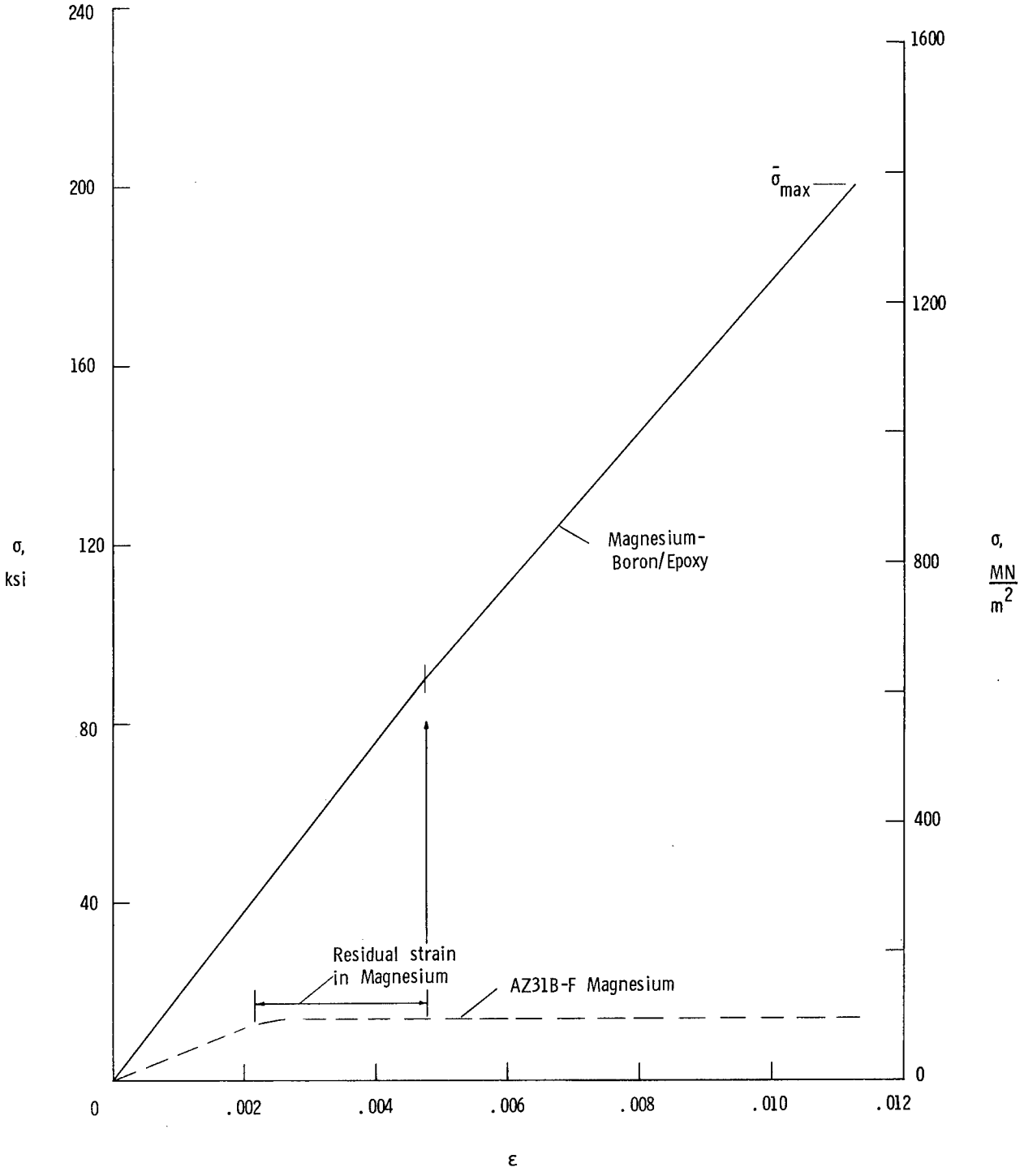

(c) Magnesium and magnesium-boron/epoxy.

Figure 5.- Continued.

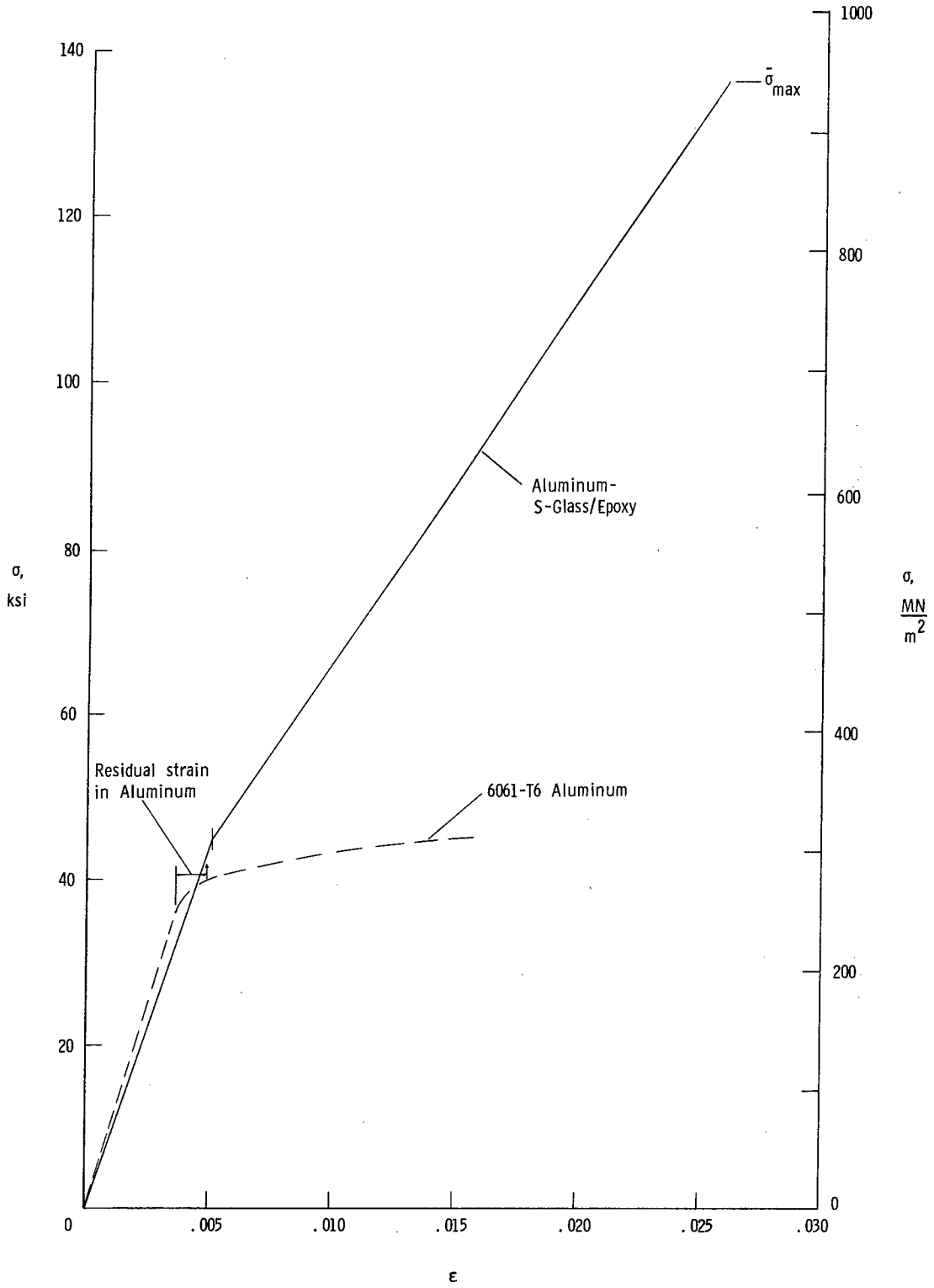

(d) Aluminum and aluminum—S-glass/epoxy.

Figure 5.- Continued.

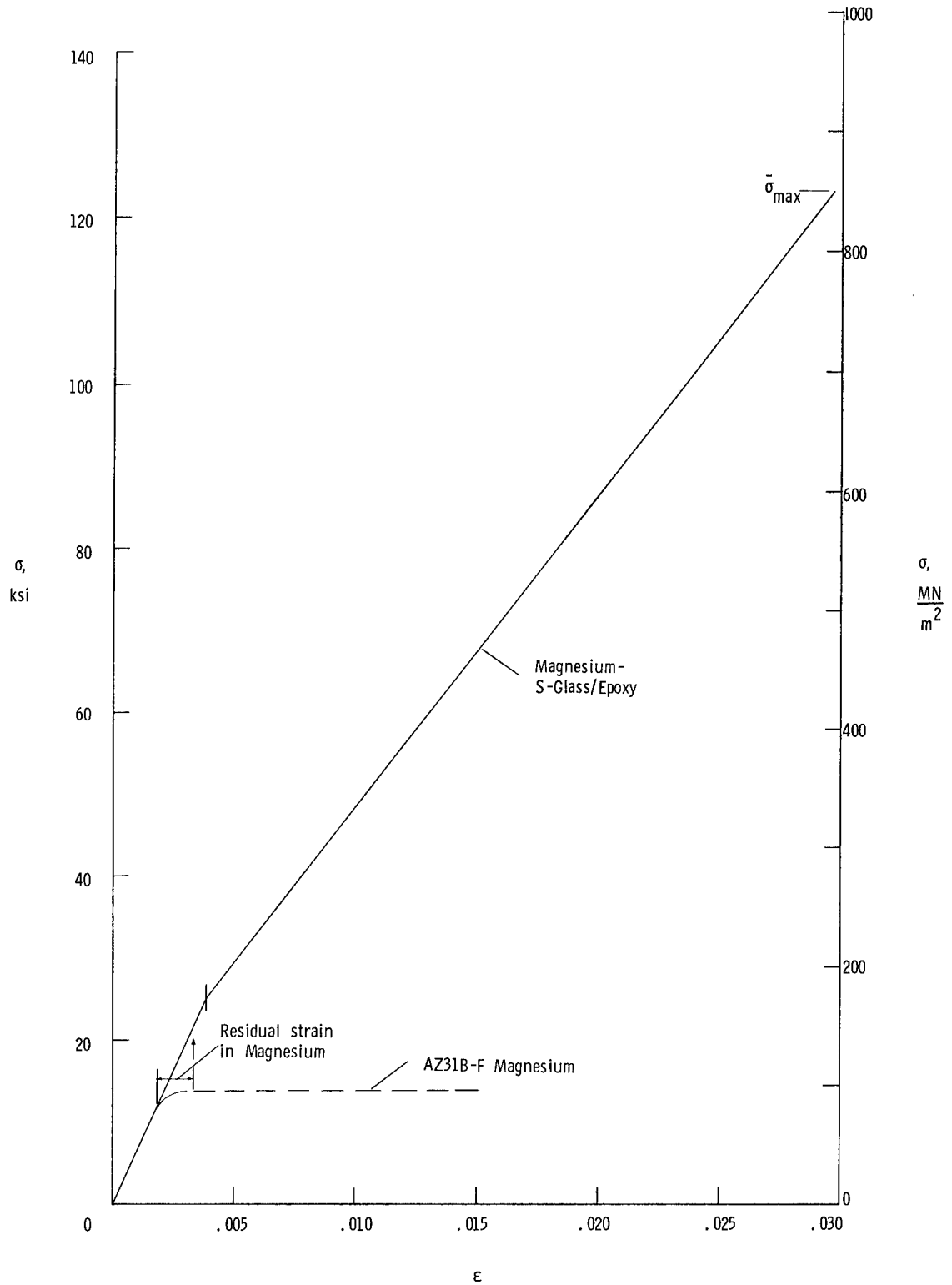

(e) Magnesium and magnesium—S-glass/epoxy.

Figure 5.- Concluded.

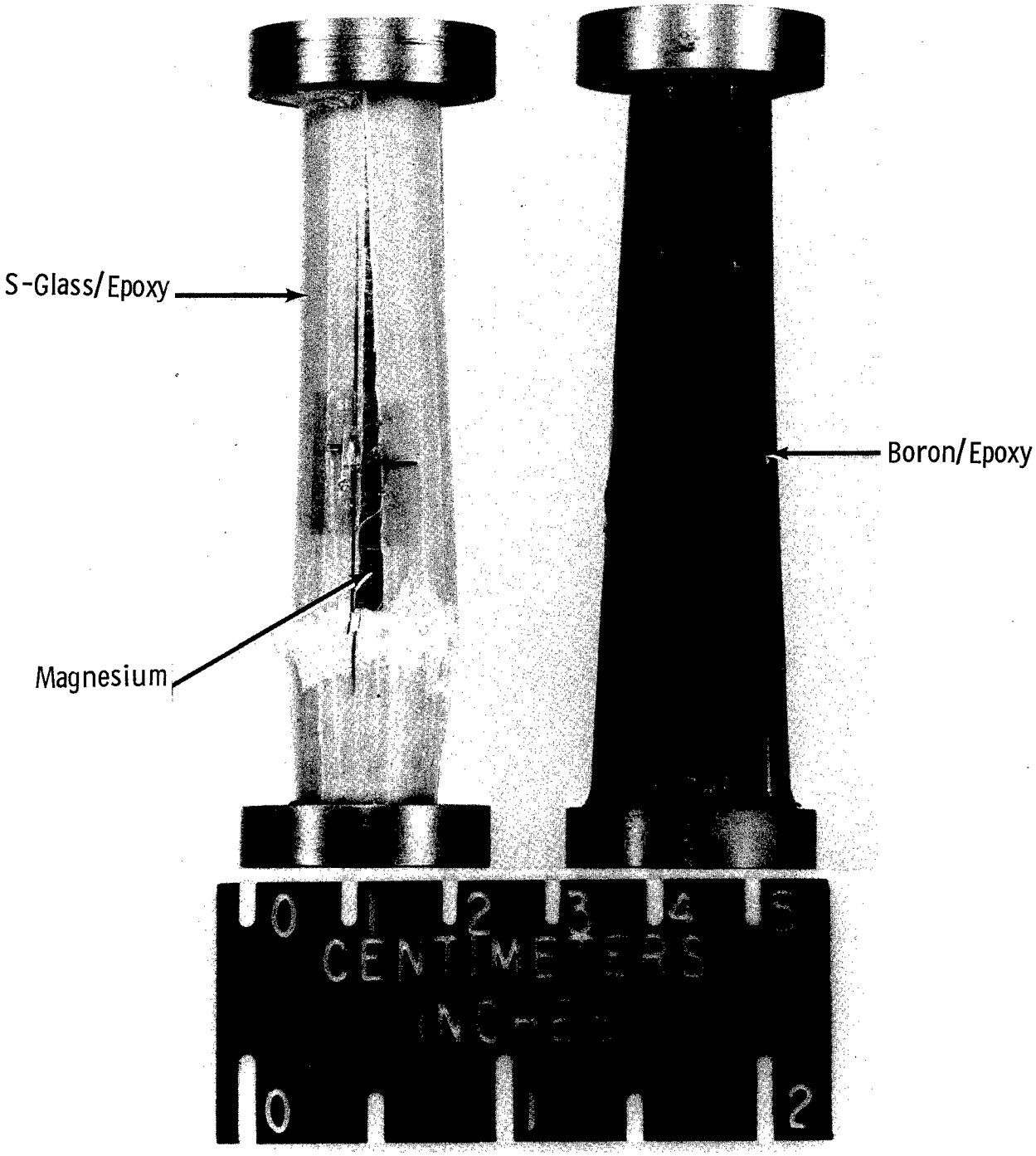

Figure 6.- Typical failures of crushing specimens. L-68-5699

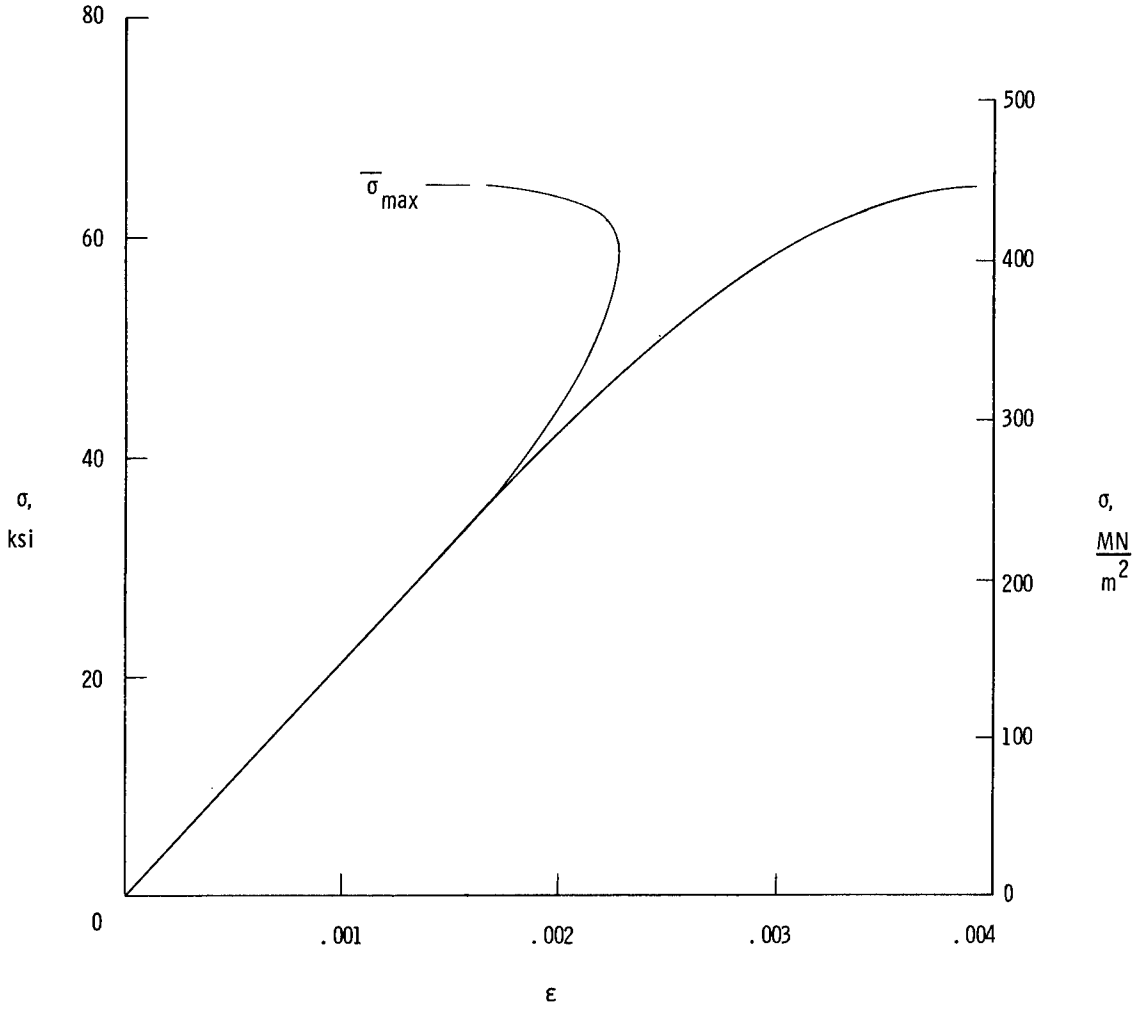

(a) Aluminum-boron/epoxy; L = 20 in. (51 cm).

Figure 7.- Typical stress-strain behavior for column specimens.

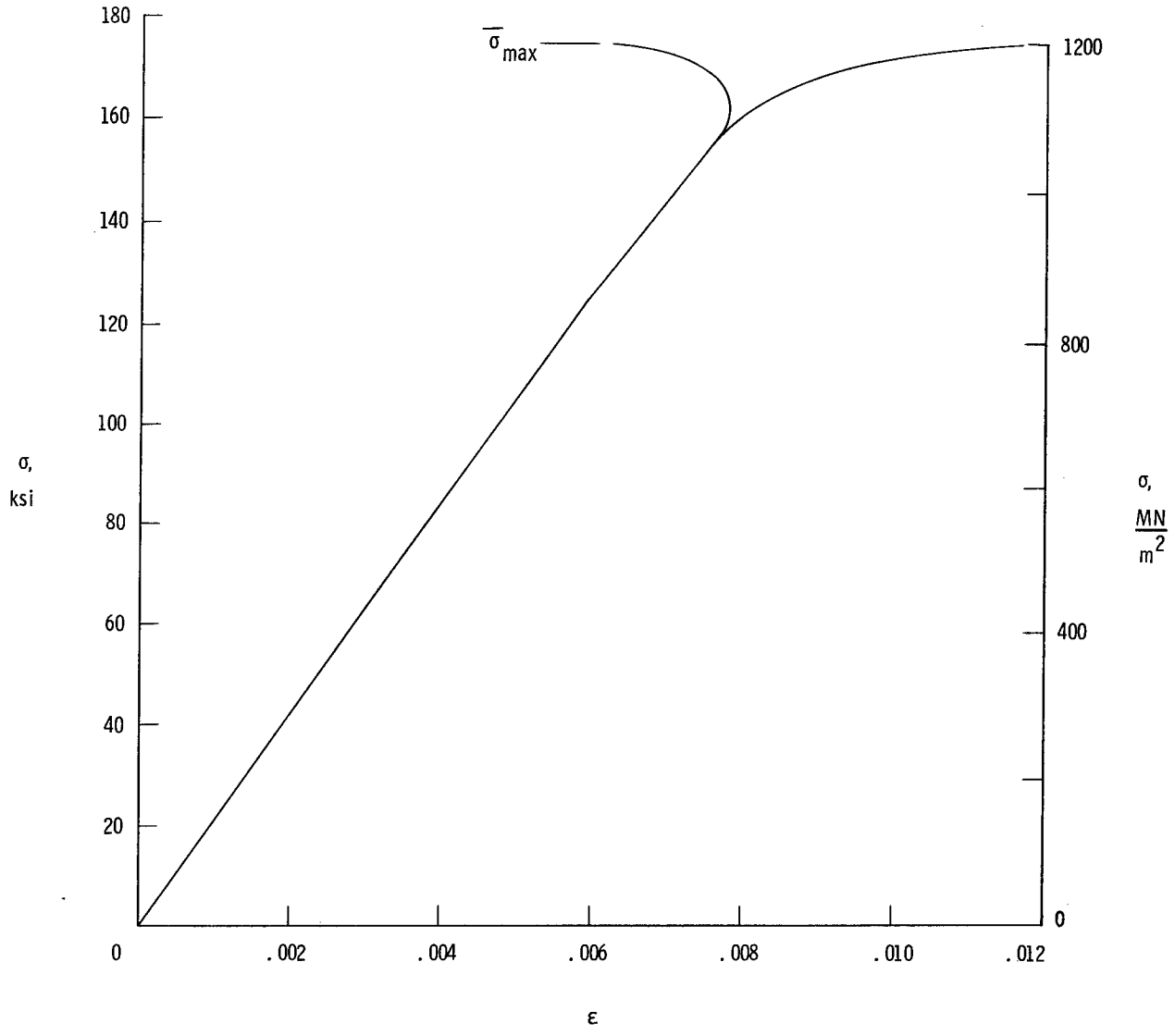

(b) Aluminum-boron/epoxy; L = 10 in. (25 cm).

Figure 7.- Concluded.

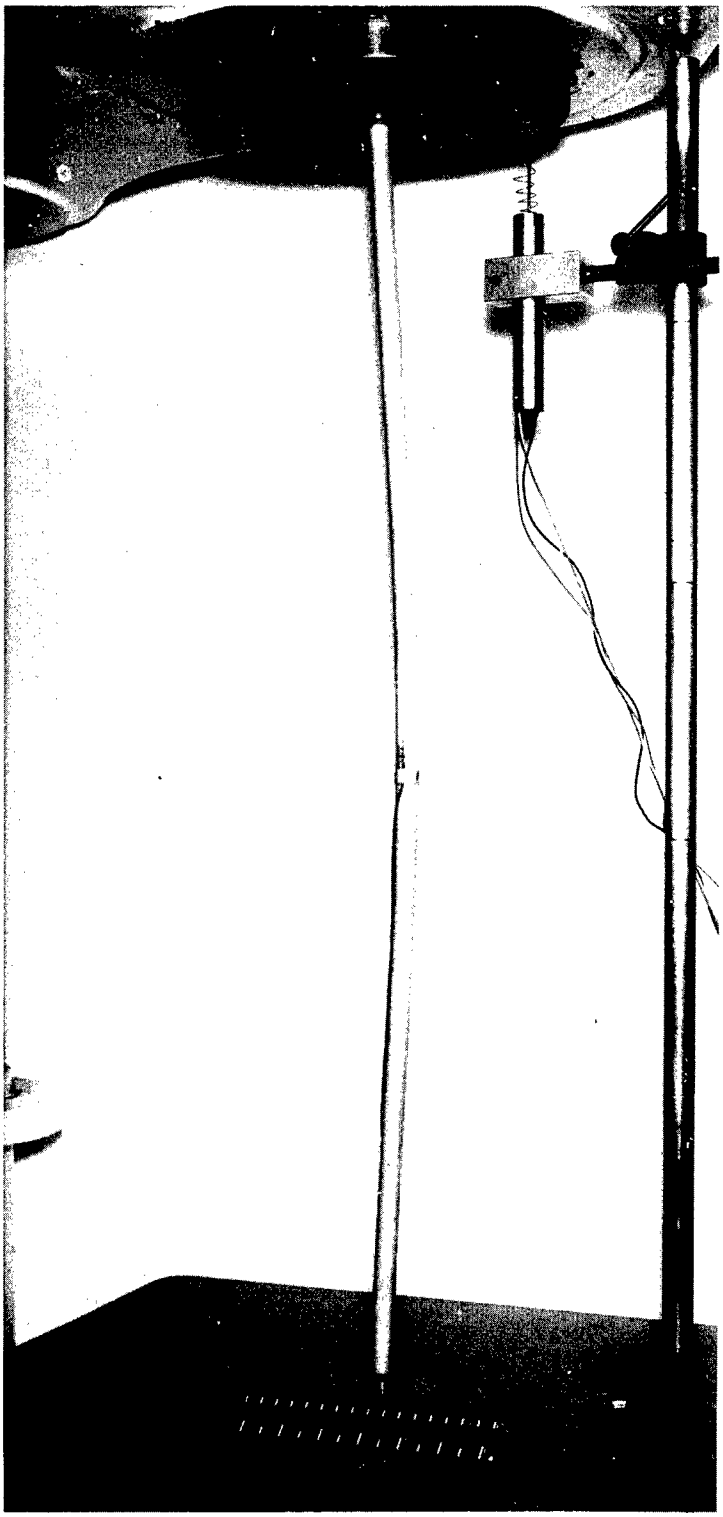

Figure 8.- Typical failure of long column specimen. L-68-5700

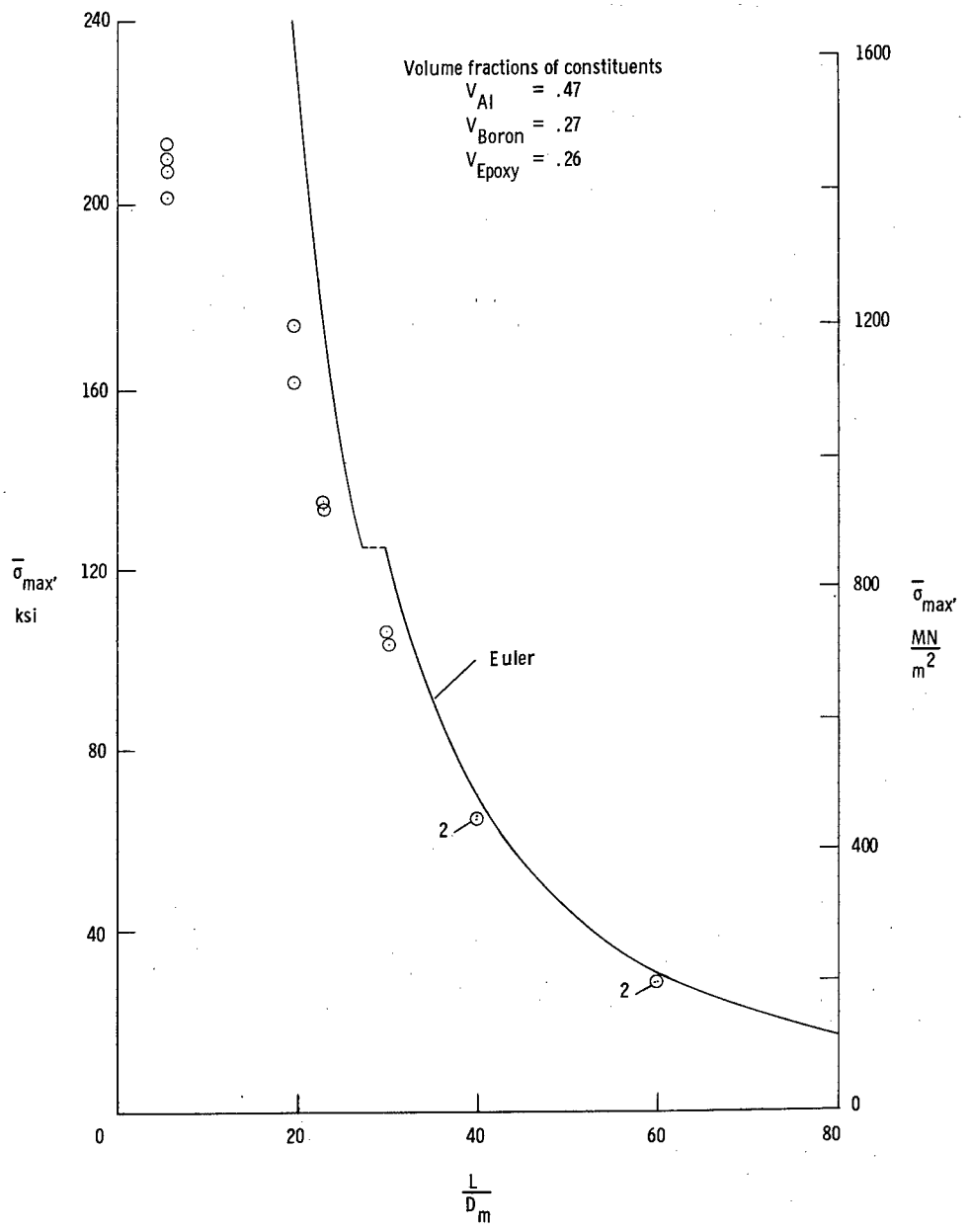

(a) Aluminum-boron/epoxy.

Figure 9.- Results of crushing and column tests for clamped-end metal tubing reinforced with filamentary composites.

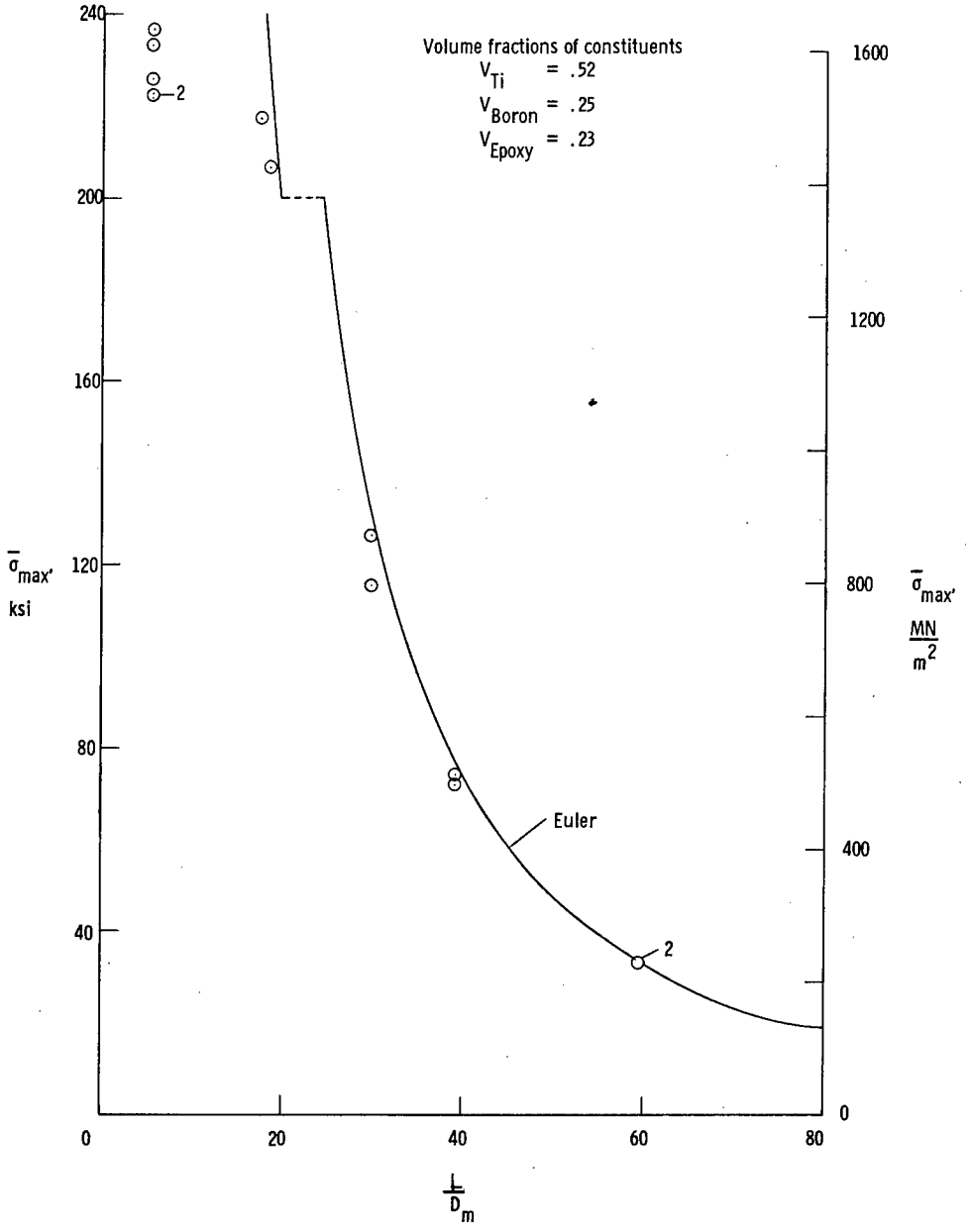

(b) Titanium-boron/epoxy.

Figure 9.- Continued.

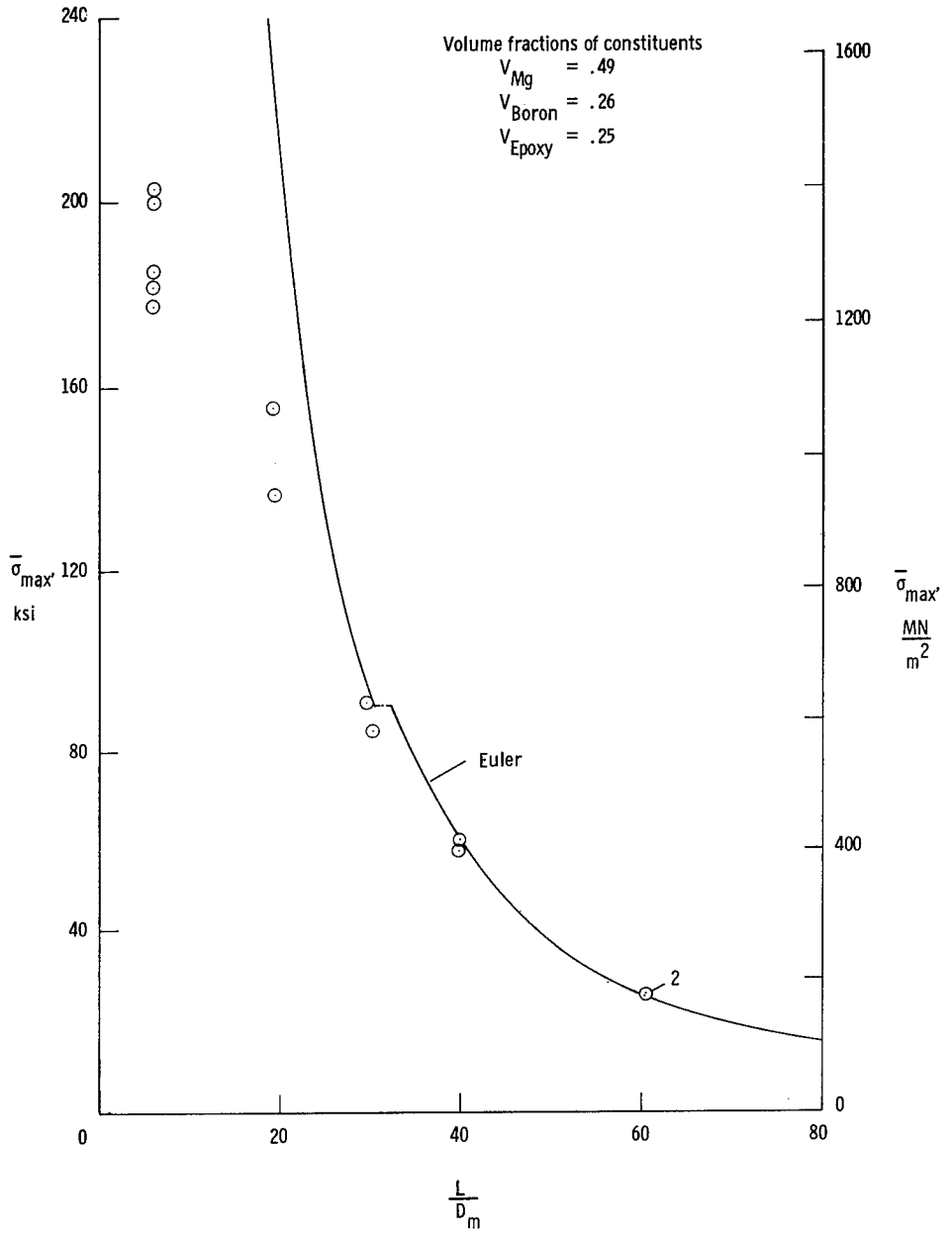

(c) Magnesium-boron/epoxy.

Figure 9.- Continued.

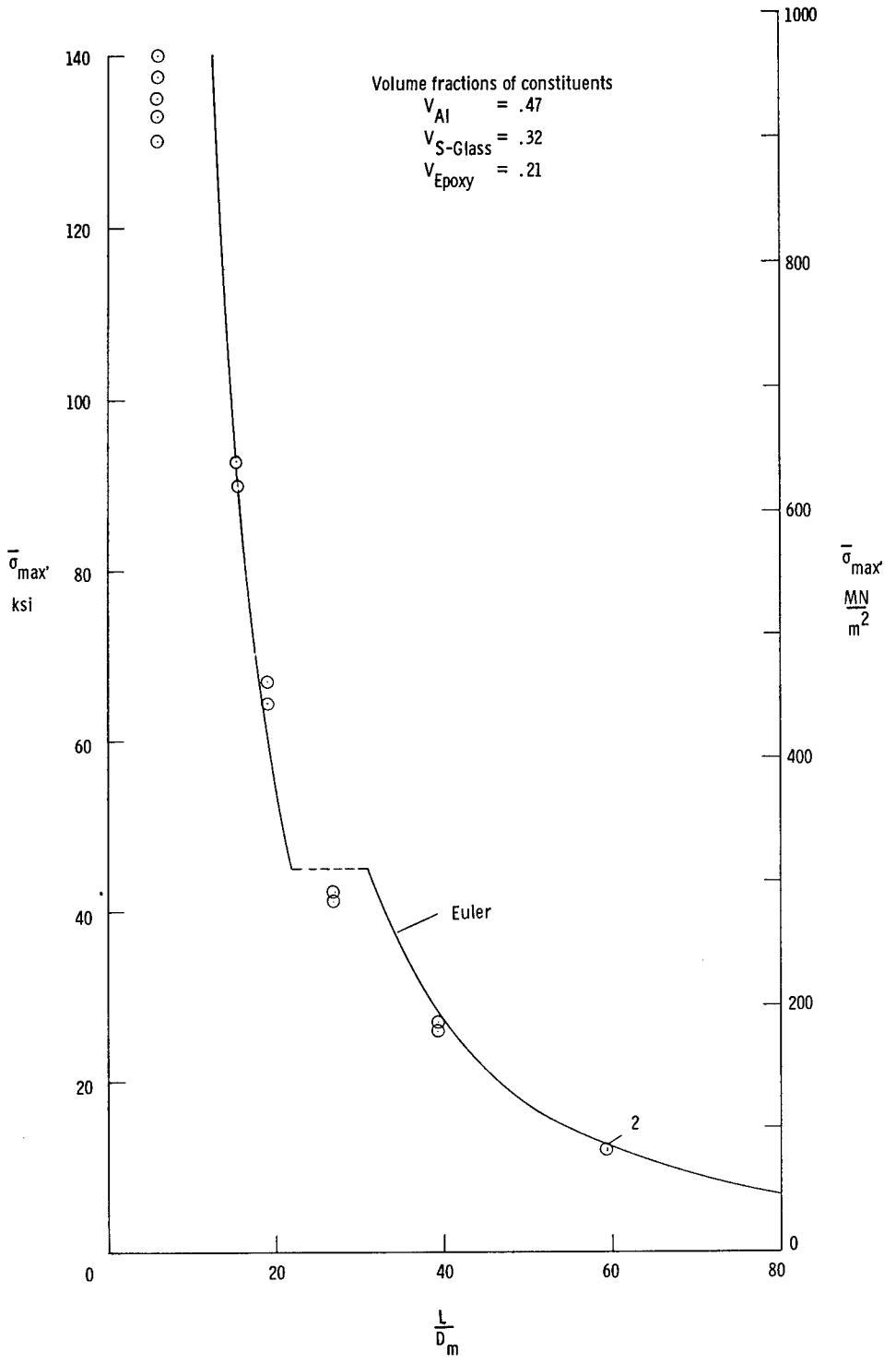

(d) Aluminum—S-glass/epoxy.

Figure 9.- Continued.

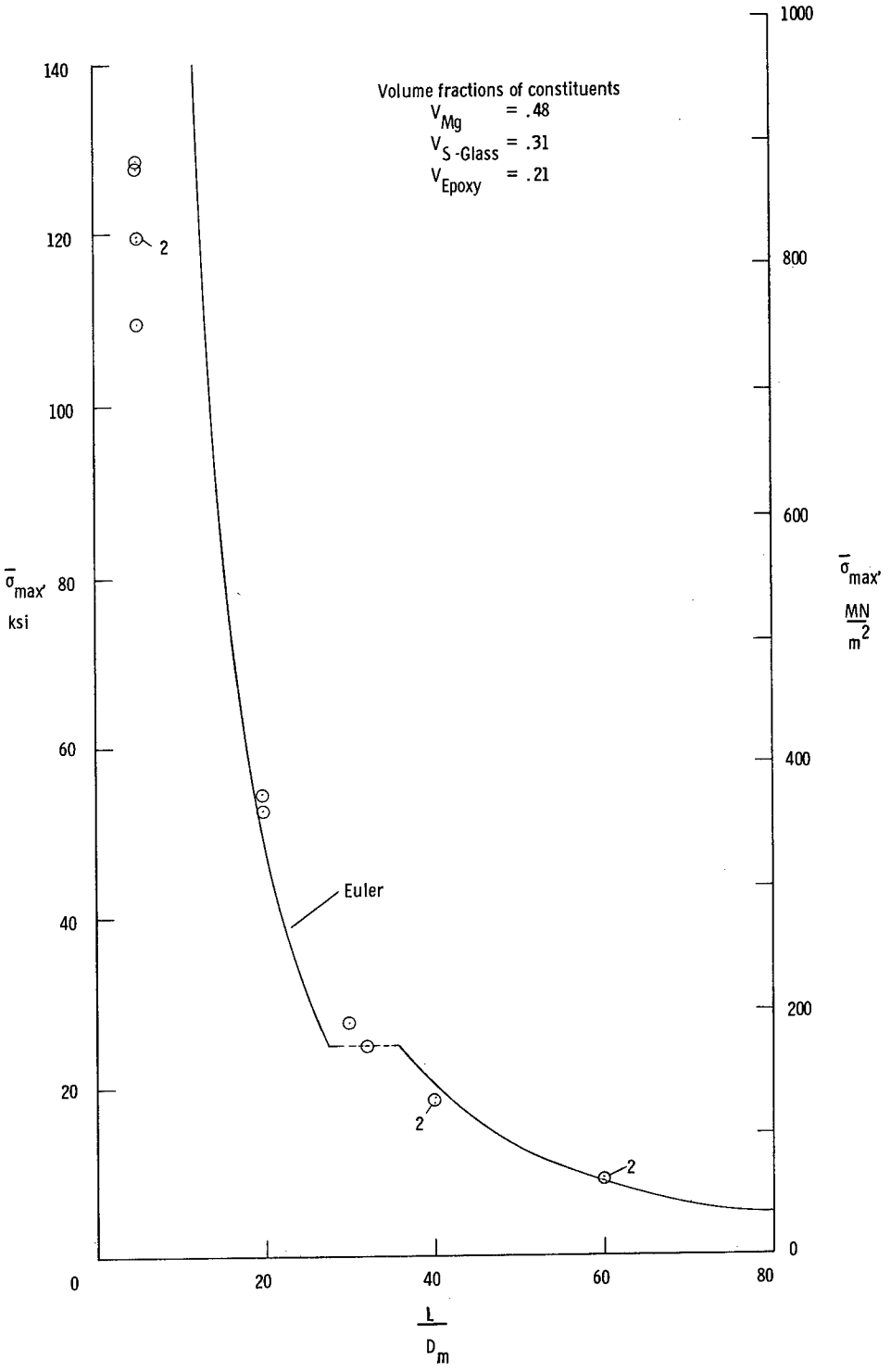

(e) Magnesium—S-glass/epoxy.

Figure 9.- Concluded.

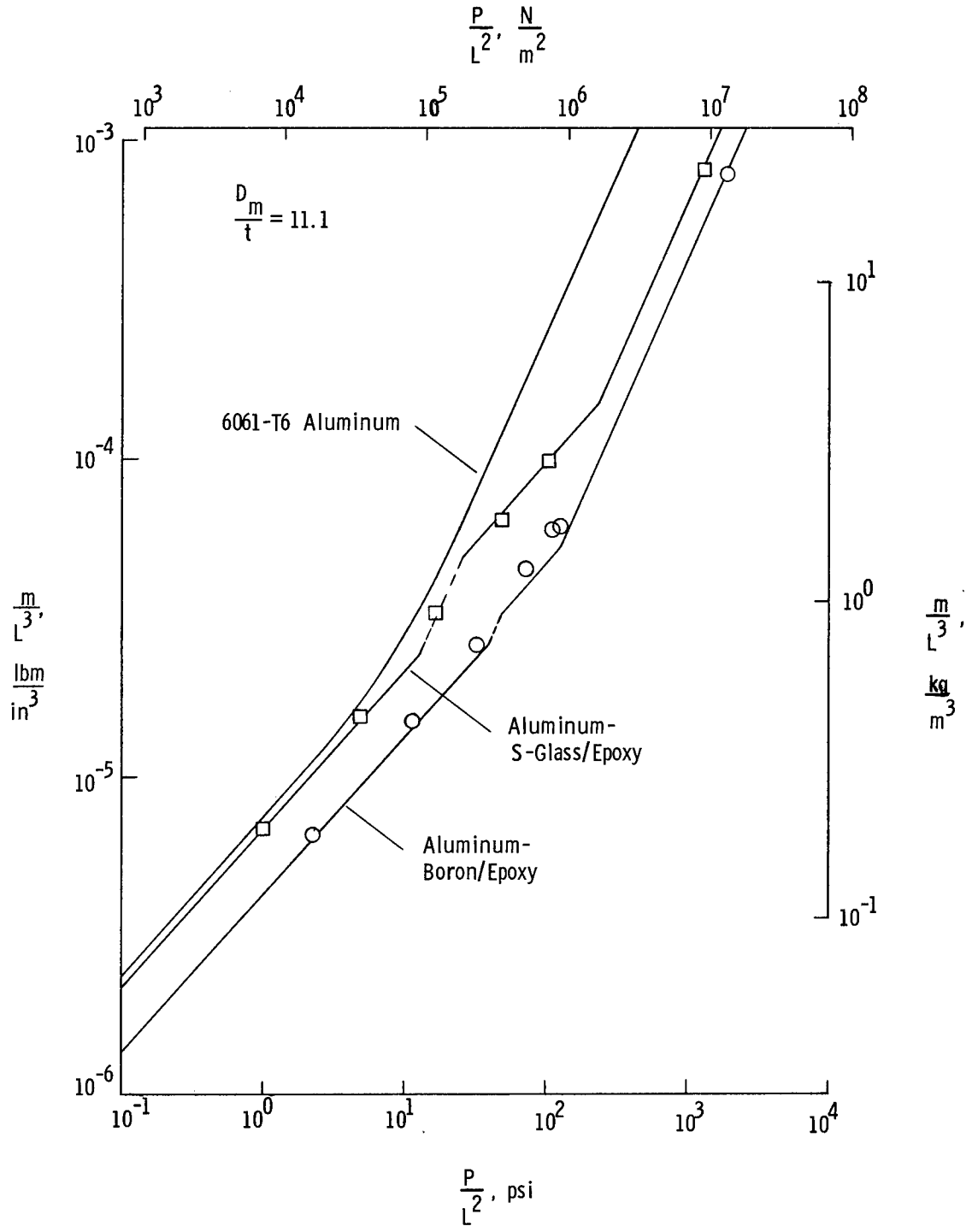

(a) Aluminum, aluminum-boron/epoxy, and aluminum—S-glass/epoxy.

Figure 10.- Mass-strength comparison of metal tubing and filamentary reinforced metal tubing.

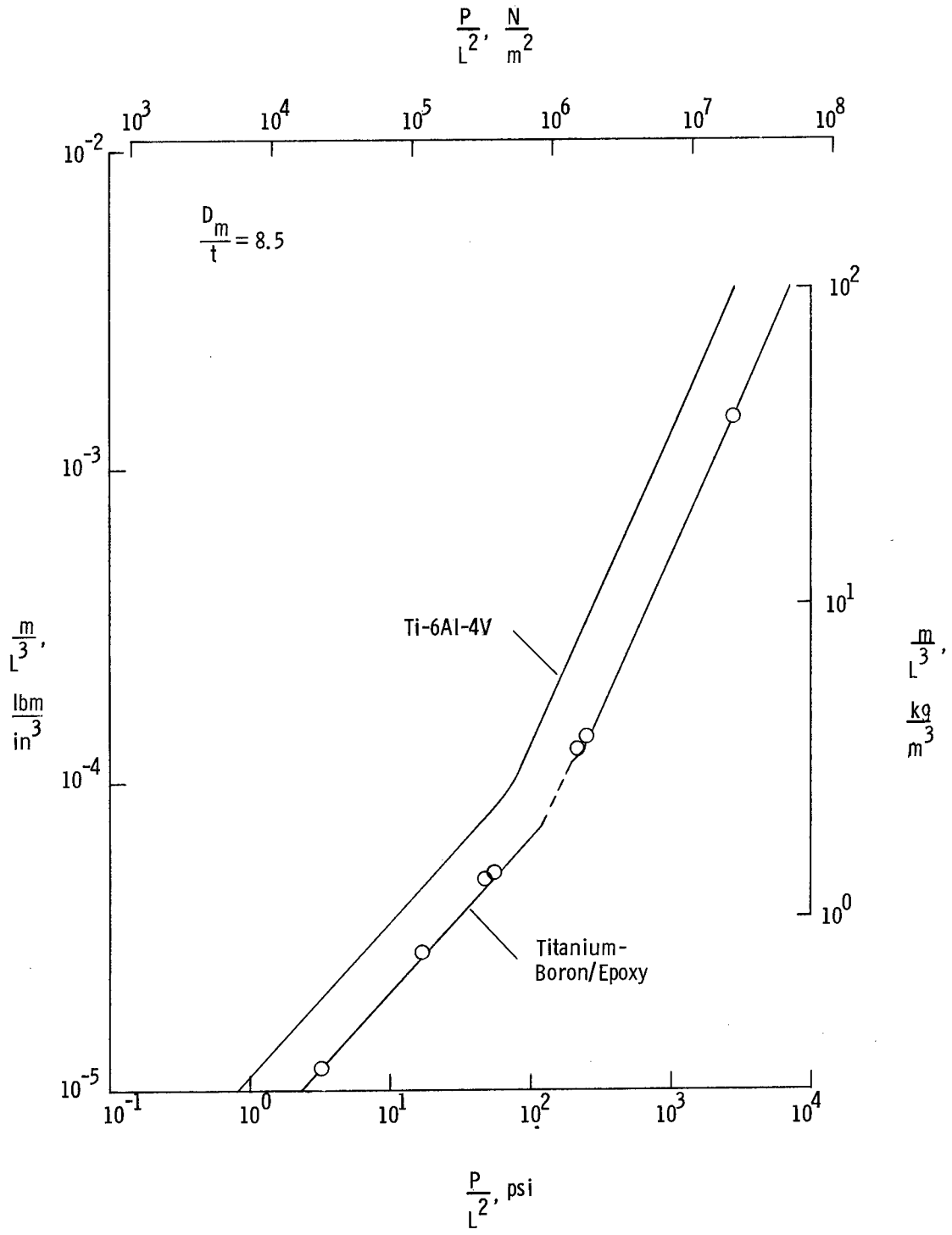

(b) Titanium and titanium-boron/epoxy.

Figure 10.- Continued.

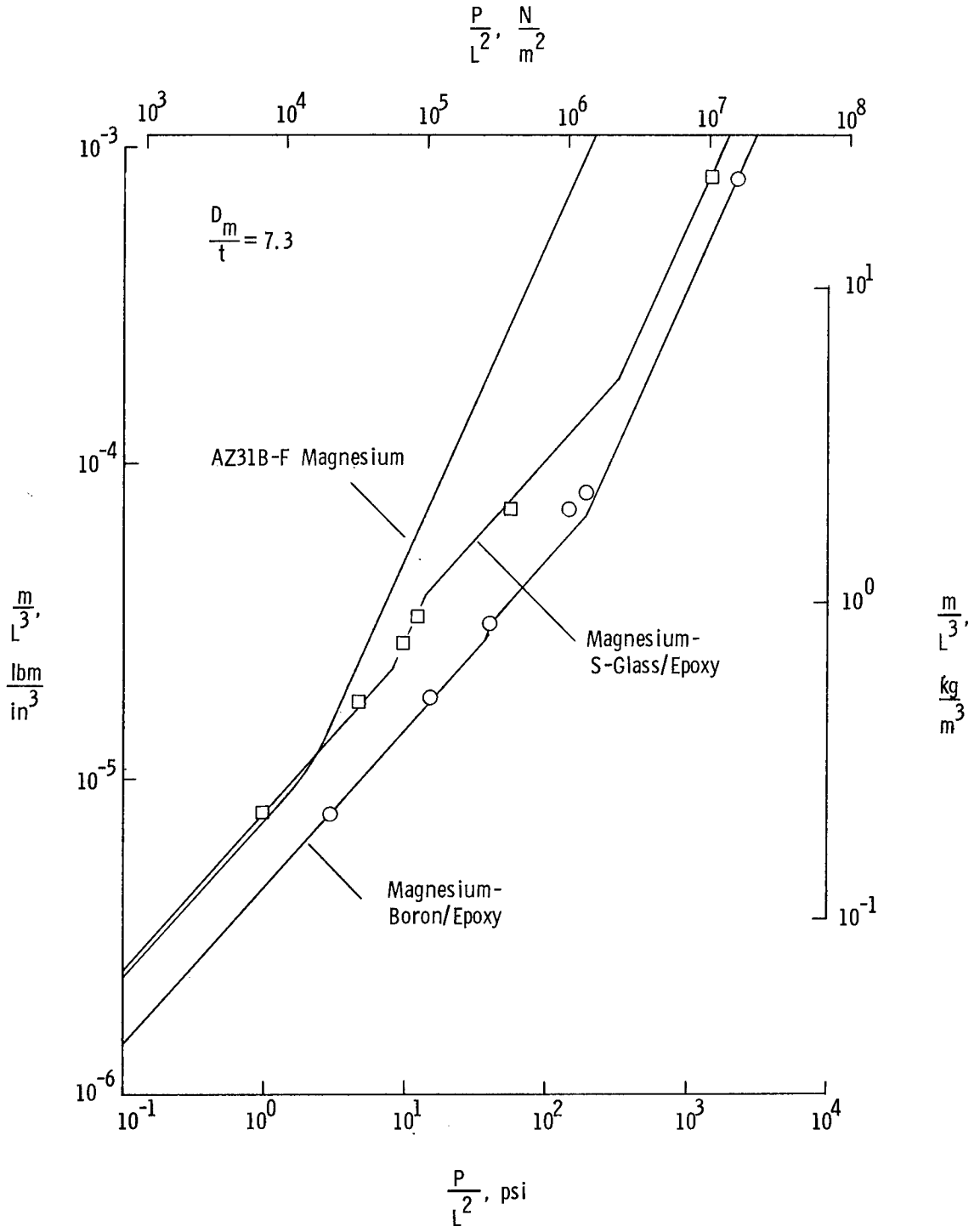

(c) Magnesium, magnesium-boron/epoxy, and magnesium—S-glass/epoxy.

Figure 10.- Concluded.

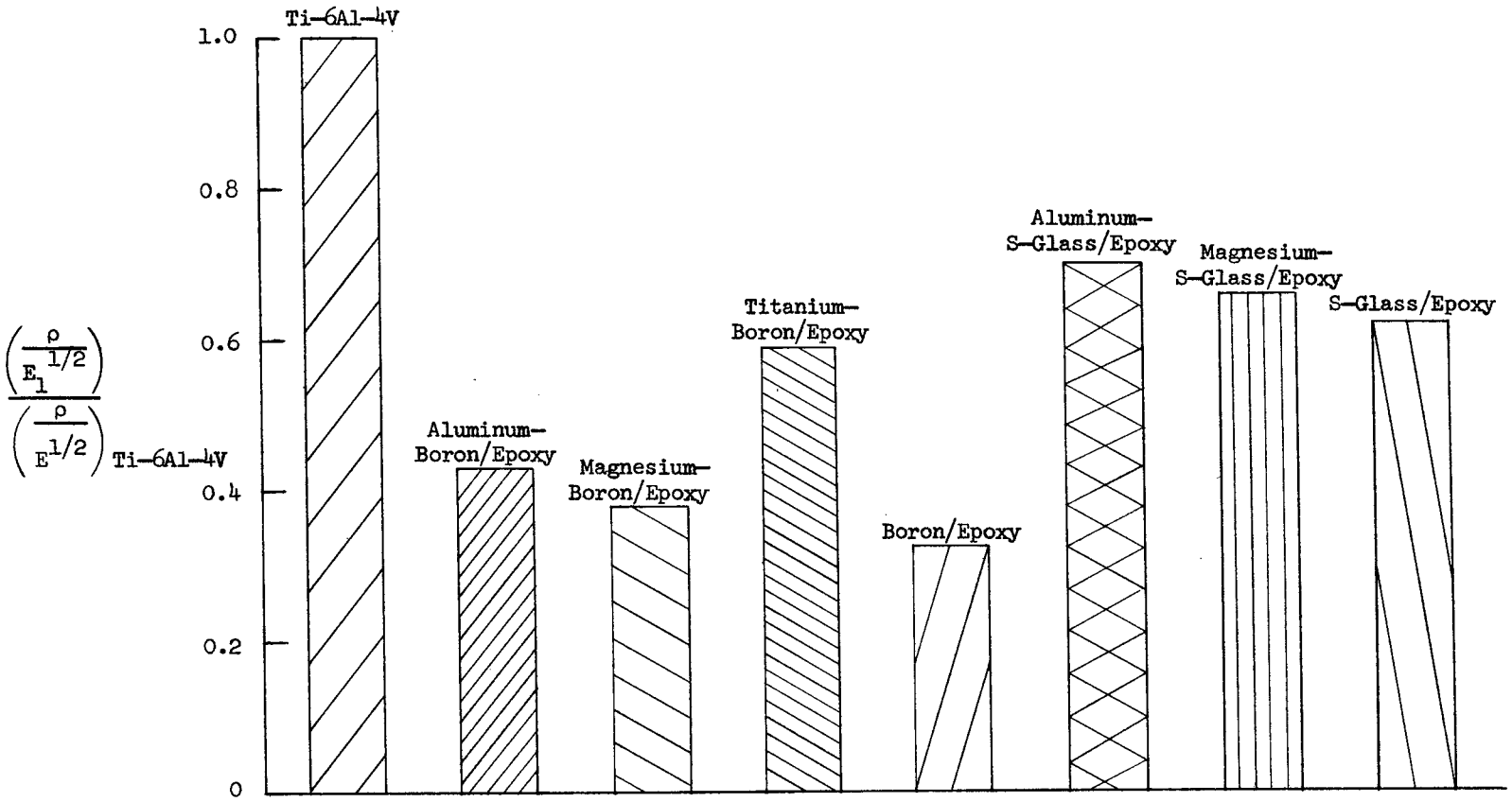

(a) Column buckling.

Figure 11.- Comparison of materials.

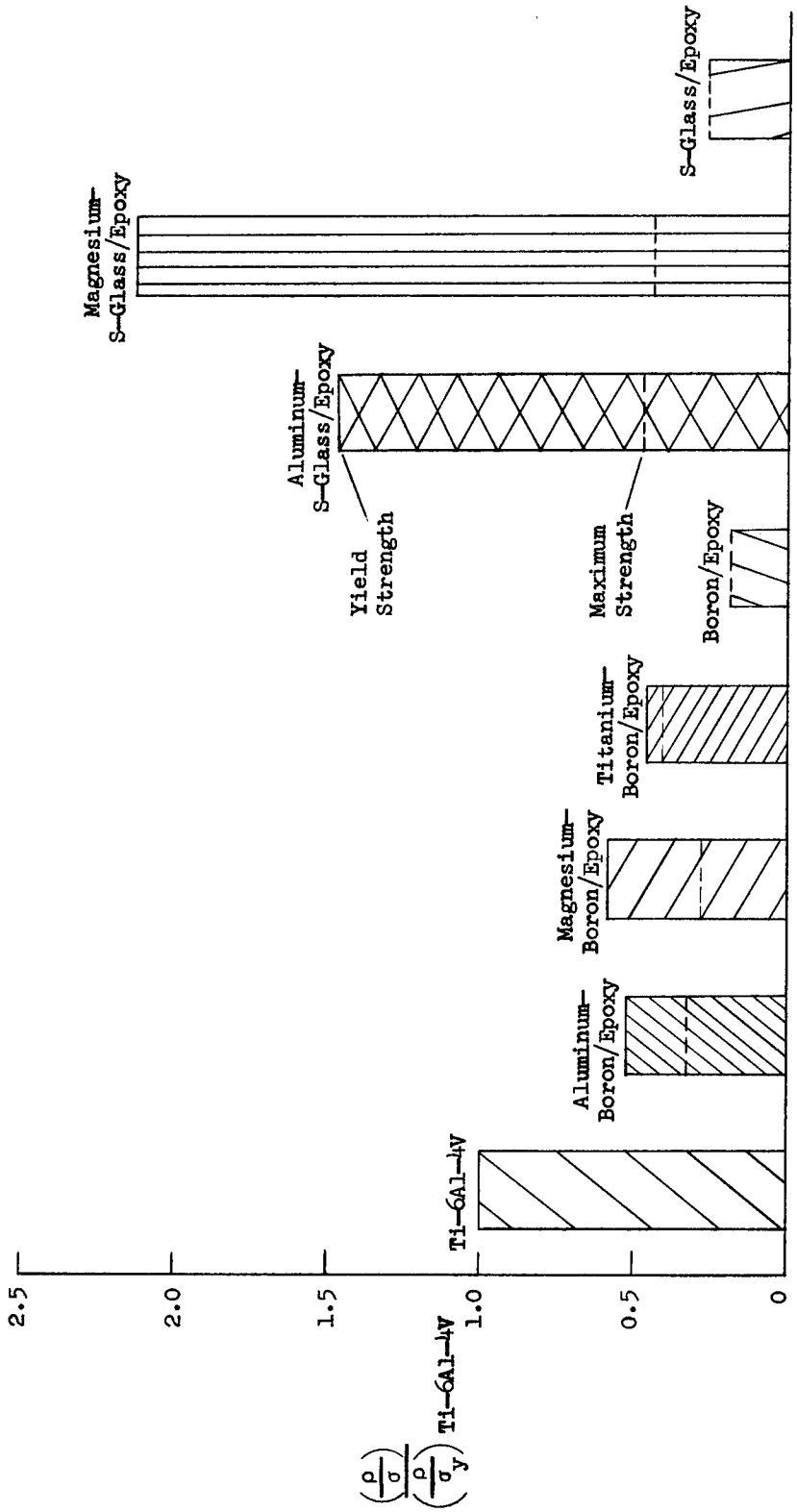

(b) Compressive yield and maximum strength.

Figure 11.- Concluded.